ENG 4001 Research Project
Miniature Underwater Drone
Final Report

Muhammad Alif Aiman Ahmad Fadzil – a1838701
Mohamad Nazif Mohammad Sobri – a1834186
Yang Li – a1781379

Professor Derek Abbott – Project Supervisor
Professor Benjamin Cazzolato – Project Supervisor

2023s1-EME.EE-DZA-UG-13492

Faculty of Science, Engineering and Technology

The University of Adelaide

October 2023

Executive Summary

This executive summary provides a concise overview of a Miniature Underwater Drone Project, focusing on the key outcomes and significance of the endeavour to develop the project.

The project aims to construct a reliable and efficient prototype underwater drone capable of conducting essential tasks in diverse underwater environments. The drone's primary functions include diving to specified depths, environmental observation using a camera, and data transmission, making it suitable for use in shallow waters and confined spaces. While initially focusing on fundamental functionalities, the project lays the foundation for future enhancements and applications.

To accomplish this, a comprehensive literature review has been conducted to understand existing projects and technologies in the field. The research has explored aspects such as radio frequency communication and underwater acoustic communication, shedding light on the challenges and opportunities in underwater communication methods.

The project progresses with a focus on both mechanical and electrical aspects. The mechanical design involves the use of an acrylic cylinder for the drone's hull, 3D-printed components for securing electronic devices, and a syringe-based control system to adjust the drone's buoyancy. On the electrical front, the project carefully designed a system that includes a Raspberry Pi 3 Model A+, pressure sensors, laser distance sensors, motors, and a camera, among other components. These components are crucial for power distribution, control, data collection, and communication with the operator.

While significant progress has been made in the mechanical and electrical aspects of the project, the project is committed to a completion plan that includes further refinement and testing. The progress will continue to iterate on the design, address any issues, and ensure the drone's stability, buoyancy, and maneuverability.

In conclusion, the development of underwater drone technology holds great promise for marine exploration and research. The project is a testament to the dedication to overcoming the challenges of underwater environments and harnessing the potential of miniature underwater drones.

Table of Contents

List of Tables

List of Figures

Contribution Statement

Student's name:

Muhammad Alif Aiman Ahmad Fadzil (Alif Aiman)

Mohammad Nazif Mohamad Sobri (Nazif Sobri)

Yang Li (Yang Li)

Table 1: Contributions statement by Role.

Role	Student
Conceptualisation	Alif Aiman, Nazif Sobri
Methodology	Alif Aiman, Yang Li
Project Administration	Alif Aiman, Nazif Sobri
Resources	Alif Aiman, Nazif Sobri, Yang Li
Software	Alif Aiman, Nazif Sobri
Visualization	Alif Aiman, Nazif Sobri, Yang Li
Validation	Alif Aiman, Nazif Sobri
Writing – draft	Alif Aiman, Nazif Sobri, Yang Li
Writing – review & editing	Alif Aiman, Nazif Sobri, Yang Li

Table 2: Contributions statement by Student.

Student	Role
Alif Aiman	Conceptualisation, Methodology, Project Administration, Resources, Software, Visualization, Validation, Writing – draft, Writing – review & editing.
Nazif Sobri	Conceptualisation, Project Administration, Resources, Software, Visualization, Validation, Writing – draft, Writing – review & editing.
Yang Li	Methodology, Resources, Visualization, Writing – draft, Writing – review & editing.

1   Introduction

In the depths of the ocean lies a world of mystery and wonder, a realm that has captured the imagination of scientists, researchers, and explorers for centuries. Yet, this enigmatic underwater world, with its vast expanses and hidden treasures, has remained largely inaccessible to human exploration due to the formidable challenges it presents. The quest to unlock the secrets of the deep has given rise to innovative technologies, and among them, the underwater drone stands as a beacon of hope, promising to unveil the mysteries of the deep while ensuring the safety of those who seek to explore it.

This report embarks on a journey into the heart of underwater exploration. The project, focused on the creation of a Miniature Underwater Drone, represents a step towards the realization of this ambitious endeavour. In the pages that follow will delve into the technical intricacies, challenges, and triumphs that have shaped the pursuit of building a reliable and efficient underwater drone.

In the following sections, essential context will be provided by exploring the background of underwater exploration and the motivations that drive the project. The project will define the aims and scope, outlining the objectives that steer the efforts toward success. The objectives, inspired by the needs of underwater research and exploration, will be clearly defined, setting the stage for the comprehensive documentation of the project's journey.

As the project navigates through the details of project, from mechanical design to electrical components and testing. The challenges the project face in designing and constructing a miniature underwater drone are matched only by the boundless possibilities it offers in terms of marine exploration, ecological monitoring, and resource development.

1.1   Background

A miniature underwater drone is a small, compact submersible designed to operate underwater. The underwater drone is made for the purpose of studying radio frequency (RF) behaviour through water. This project was inspired by the Lego-powered Submarine from the Brick Experiment Channel on YouTube, as shown in Figure 1. The Lego-powered Submarine project started due to the issue of maintaining a constant depth for a remote-control submarine [1]. The creator decided to implement PID control and utilized the pressure sensor by using a Raspberry Pi as a microcontroller to measure the depth [1]. The problems encountered in the channel were that the end caps for the submarine were hard to close, the propeller didn't turn strongly, and the submarine was unable to maintain a straight course when it reached its peak speed [1].
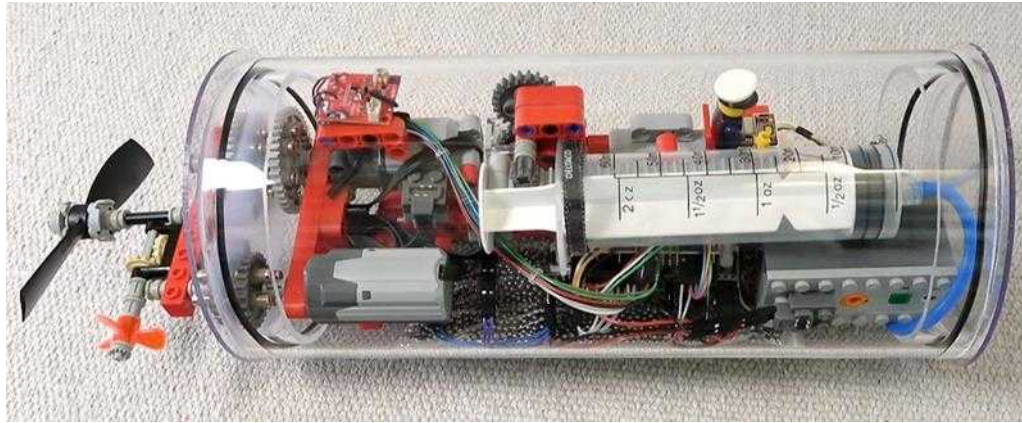
Figure 1: Lego-powered Submarine from Brick Experiment Channel [1].

1.2 Motivation

The origin of the project was inspired from an existing project from the "Lego-powered Submarine" project by the Brick Experiment Channel [1]. While drawing inspiration from existing projects, the project's core motivation lies in advancing the capabilities of underwater exploration. The project recognizes the immense potential of underwater drones in scientific research, environmental monitoring, industrial applications, and education. The motivation for the project arises from the recognition that there is a pressing need for efficient, cost-effective, and versatile alternatives to conventional underwater exploration methods. The vast potential of underwater ecosystems, resources, and geological formations remains largely untapped due to the inherent risks and limitations associated with human intervention.

1.3 Aim and Scope

The project aims to design, construct, and deploy a Miniature Underwater Drone that will serve as a technological solution to the challenges of underwater exploration. This drone will be equipped with a range of sensors and cameras to provide high-precision perception of the underwater environment. By leveraging state-of-the-art technology, the project intends to enable this remote-control drone to conduct tasks in underwater environments, thus minimizing human exposure to risks and expanding the capabilities in marine scientific research, resource exploration, and environmental protection.

1.4   Objectives

Miniature Underwater Drone primary objective is to develop a reliable and efficient prototype. To achieve this objective, the project will employ 3D printing technology for the construction of the Miniature Underwater Drone's physical components. 3D printing offers advantages such as rapid prototyping, customization, and cost-efficiency. The design and manufacturing process will adhere to best practices to ensure optimal underwater maneuverability and stability.

The next objective for the project is to develop and integrate RF control system. The project will involve the development and integration of an RF control system. This system will be based on the Raspberry Pi Model 3 A+, serving as the microcontroller for the Miniature Underwater Drone. The RF control system will enable wireless communication between the operator and the drone. The Raspberry Pi will be programmed to manage commands from the operator and translate them into actions for the drone's propulsion, navigation, and data collection subsystems.

To achieve the critical objective of enabling the Miniature Underwater Drone to dive to designated depths, a comprehensive approach must be undertaken. This entails the design and implementation of a depth control mechanism, potentially utilizing adjustable ballast or variable buoyancy systems, thereby enabling the drone to autonomously manage its depth. Additionally, the integration of depth sensors or pressure sensors is essential to furnish real-time depth data to the control system. To effectively control the drone's buoyancy and maintain the desired depth.

Environmental observation is a critical aspect of the Miniature Underwater Drone's functionality. To achieve this objective, the project will incorporate a camera system into the drone's design. The camera system will be equipped with high-resolution imaging capabilities, allowing it to capture clear underwater footage. A live video feed will be transmitted to the operator's control station, facilitating environmental monitoring and observation.

1.5   Document Overview

This report provides a comprehensive account of the project's journey, from inception to implementation. It encompasses a detailed literature review, outlining the technical background and challenges associated with underwater exploration and drone technology. The report delves into the approach and methods for building the Miniature Underwater Drone, covering both mechanical and electrical aspects.

The updates on the project's status can be found as the project progresses, including advancements in the mechanical and electrical components. The project's completion plan outlines the stages it will undertake to refine and test the drone further. Finally, the report concludes with insights into the significance of the project within the broader context of technological innovation in underwater exploration.

2   Literature Review

The field of underwater exploration has witnessed remarkable advancements in recent years, driven by the need for efficient and secure data collection in the most challenging marine environments. In this section on underwater drone technology will delve into the significant developments, with a particular focus on related projects. As advancements are explored, it becomes evident that autonomous underwater vehicles (AUVs) and remotely operated vehicles (ROVs) play pivotal roles in pushing the boundaries of what's possible beneath the waves. In this literature review, key developments have been examined in underwater drone technology, focusing on existing projects.

2.1   Autonomous Underwater Vehicles (AUVs)

Autonomous Underwater Vehicles, commonly referred to as AUVs, are self-propelled, unmanned devices designed for underwater exploration and data collection [6]. These vehicles operate autonomously, following pre-programmed missions or making real-time decisions based on sensor inputs enabling comprehensive data collection about the underwater environment [6]. AUVs have a wide range of applications, including oceanography, marine biology, environmental monitoring, and underwater archaeology. AUVs incorporate several key components for effective underwater exploration. In the pursuit of efficient underwater movement and precise control, AUVs incorporate a range of key components. These include various propulsion systems, such as thrusters or propellers, which facilitate efficient locomotion, enabling precise control of both speed and direction [6]. This aspect aligns with the relentless need for sophisticated technology to navigate the often-challenging underwater landscapes [6].

Figure 2: The UK Natural Environment Council (NERC) Autosub6000 AUV [6].

2.2 Remotely Operated Vehicles (ROVs)

Remotely Operated Vehicles (ROVs) is an unmanned underwater vessel are typically operated through what is referred to as the "umbilical cable" [7]. This cable is a critical lifeline for ROVs, providing both a high-bandwidth low-latency communication link and a power supply, facilitating real-time remote operation [7]. However, this tethered setup inherently limits the mobility of ROVs due to the risks associated with cable strain and entanglement. For specific ROV applications, such as under-ice research or missions in high-risk environments where tether entanglement is a concern, the presence of on-board batteries offers a distinct advantage. In emergencies where cutting the tether is necessary, medium, and small-size inspection-class ROVs can safely resurface, essentially functioning as AUVs. Underwater wireless communication can be established through different technologies, including radio frequency (RF), optical, and acoustic modems. These technologies offer varying performance characteristics and are suited to different types of applications [7]. RF and optical communications are capable of delivering short-range broadband communication links, while acoustic signals excel in long-range, low-rate communications. Combining these technologies into underwater multimodal networks allows for adaptable underwater communication [7].
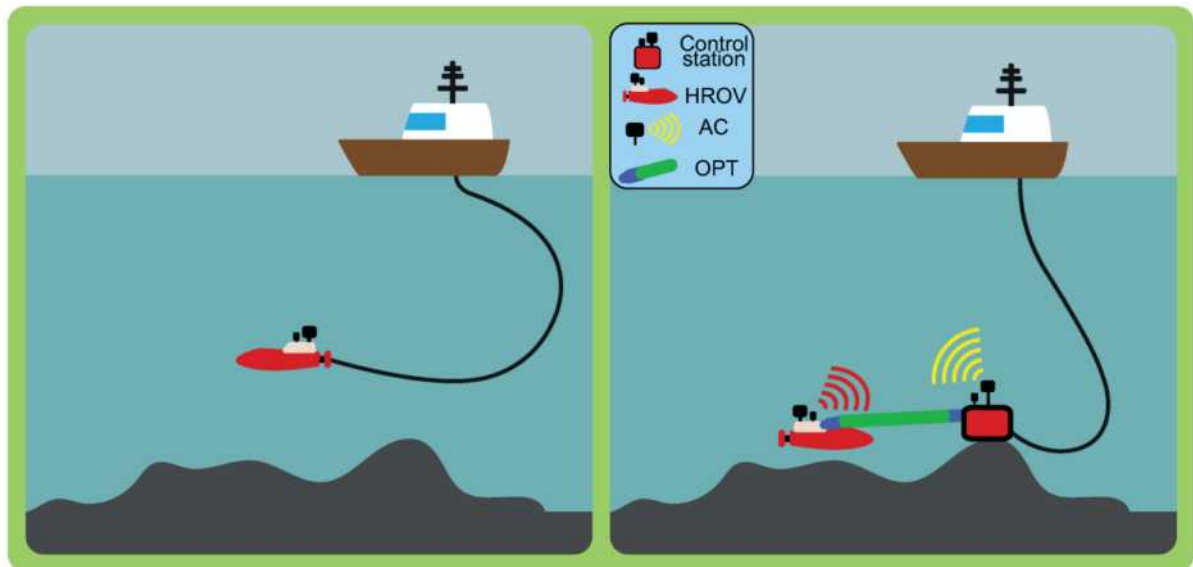
Figure 3: Comparison between a wired (ROV) and a wireless ROV control [7].

3   Methodology

This section provides a comprehensive overview of the systematic methodologies applied during the design and development phase of the underwater drone and presents an in-depth analysis of the strategies employed throughout the project making. All specifics in Section 3.1 are sourced from datasheets referenced as [12] to [19].

3.1   Hardware, Components and System Development Process

3.1.1   Buoyancy and Depth Control

The syringe is a medical syringe that was bought from a local medical instrument store. The capacity of the syringe is 60ml, which means the buoyant force it could produce is 0.3N. Though more capacity could provide safety in case the hull leaks, the hull size limited the size of the syringe. The length of the fully extended syringe is 26 cm. Since a little space was needed at the front of the syringe to allow a pneumatic hose to be installed and the length of the hull was 26cm, the bottom of the syringe plunger was cut off to reduce the length by 0.5cm, which can be referred to Figure 4. To make it possible to move the plunger in both directions, similar methods were used as the Lego RC Submarine Project. In that project, two rack-gear pairs and other Lego components were used to adjust the plunger position to control the diving procedure. In this project, a pair of rack-gear structures were designed using software similar with the Loge components and 4 copies of the rack-gear were 3D printed. These racks were attached at all sides of the plunge by using super glue and were clamped by four gears installed on 2 printed 5mm diameter shafts as shown in Figure 5. Since the shafts are needed to transmit large torque to the gears, superglue was used to reinforce the connection between them.

Figure 4: The bottom of plunger.
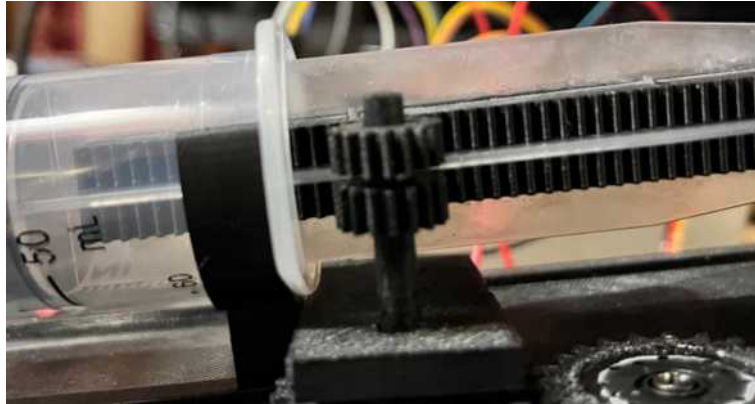
Figure 5: Racks clamped by gears.

To transmit the power from the servo motor to the gears on the syringe, three 3cm diameter gears were attached to a 3D printed board as depicted in Figure 6. In order to fit the gears on the axis they should be, there is a 2cm hole on one of the 3cm gears to fit it on a 2cm diameter round disk on the servo motor, and the other two gears were drilled a 5mm hole in the middle. These two 3cm gears are on the same shafts as the syringe gears. At the beginning the servo motor was planned to be installed on the bottom of the drone, which is the same side as the syringe was placed. It was found that the servo motor was too high to be placed at the bottom. Thus, a hole is drilled on a 3D printed board, which carries all the electrical components and physical structures in the middle level inside the drone, to install the servo motor on the top, while the gear and motor disk was installed on the bottom side of the board.
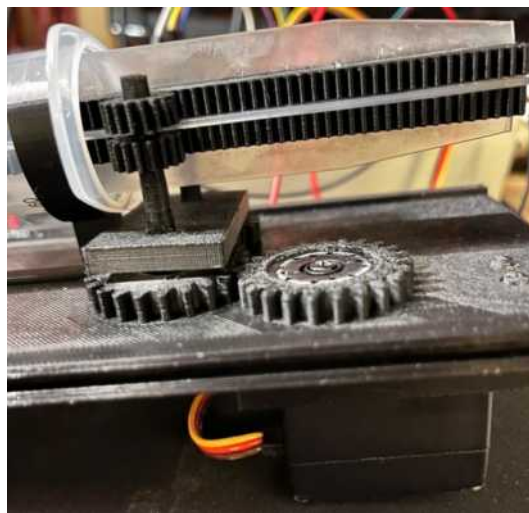
Figure 6: 3cm gears to transmit power.

3.1.2 Pressure Hull

The Pressure Hull of the drone should be rigid and transparent. Firstly, a rigid hull can prevent itself from being compressed too much by the water pressure, and then lose the allowed 0.3N buoyancy force produced by the syringe. Secondly, a transparent hull can provide a clear view of the inside, which would help to make solving problems much easier by observing the actions of all components inside.

Though a narrow hull is better at faster movements, the hull is still chosen to be flat on both sides because a camera was planned to install in the front of the drone, and magnets were used to transmit power through the hull without drilling any holes. As the Lego RC Submarine Project used a 110mm outer diameter tube as the hull, a same size tube was chosen in this project for comparison.

The hull of the drone was constructed with one 260mm long acrylic tube with 110mm outer diameter (OD) and 104mm inner diameter (ID), one 45mm long acrylic tube with 100mm OD and 95 mm ID, and a 2mm thick A4 size acrylic sheet. To cap both sides of the 260mm length tube, the 45mm tube was cut into two 20mm long tubes and the sheet was cut into two circles with 120mm diameter. These laser-cutting jobs were provided by the labor force at the university. To stick the sheets and tubes together, acrylic adhesives such as ACRIFIX were used to stick them together as well as seal the caps shown in Figure 7.

Figure 7: Acrylic adhesive and glued cap.

Since there is a 2mm gap between the 100mm OD cap and the 104mm ID cylinder, two 2.5mm thick rubber O-ring cords were used on both sides of the hull. To ensure sufficient stress to hold the O-ring on the cap and the cord could fit into the smaller gap with enough thickness, the length of the O-ring cord was 267mm, which was 15% shorter than the perimeter of the 100mm diameter outer surface. To make the cord into an O-ring, both sides of the cord were glued together with super glue on an angle iron surface. This could reduce the possibility of misalignment, which could lead to water leakage. To connect the syringe ballast and sensors inside the hull, two 3.5mm holes were drilled on the rear cap, which is defined by the place installed the propeller. Since the diameter of the pneumatic hose is 4mm, to fit the hoses into the holes, one side of the hose was sharp to make sure it could be easily pushed into the hole.

According to the Buoyancy Formula, to dive the drone under the water, the counterweight needed was 2780 grams, and the weight of the drone was 826 grams. Thus, the counterweight needed is 1954 grams. Though tungsten was chosen to be the counterweight in the Lego RC Submarine Project, due to its expensive price lead was chosen instead in this project. Lead is cheaper and still has a density of 11.3 g/cm^3 [8]. The counterweights were placed at the bottom of the drone to decrease the height of the center of gravity, so that the drone would not flip upside down.

3.1.3   Propulsion System

The 3D models of the propellers were downloaded from a free website, while others were made with Fusion 360. These propellers are then drilled to fit in the shafts. There are two propellers on the drone, one is for turning and the other is for thrusting, which can be seen in Figure 8. The thrusting propeller is placed on the middle axis of the whole drone to make sure that the force does not produce torque which is likely to turn the whole drone. The turning propeller is aligned with the thrusting propeller to prevent pith motions.

To transmit the power from the motors inside the hull to these propellers outside, Neodymium magnets pairs were used. Neodymium magnets could provide larger force compared to other magnets, and with the use of magnets less holes would be drilled on the hull, which reduced the likelihood of water leakage. The use of magnet pairs can transmit more torque through the sheet comparing to placing same poles on the same side. When the gears are turning, the magnets will push the different poles at the other side of the sheet instead of shifting to the next attracting pole. In the Lego RC Submarine Project, the magnets is fitted inside the gears by wrapping tapes around the magnets then push them inside. Because of the huge manual difficulties of this method such as

wrapping tapes on a small magnet, 1mm thick iron sheets was used to attract the magnets to hold them in position, and the sheets are installed on the same shafts together with the gears that the magnets are fitted in. The sheet is cut circularly with a water-cutting machine, and the hole at the middle of the sheet is the same as the centre hole on the gears.

For turning the gears on the cap with less friction, Ultra-High-Modular-Weight (UHMW) tape was used on both sides of the caps between the gears and the acrylic sheet. The reason this material was chosen is that it has the lowest friction coefficient around 0.1 according to CurbellPlastics [9] and it was relatively easier to buy. Moreover, silicon spray was used both on the tapes and the magnets to reduce the friction further, because the torque produced by motors is insufficient.
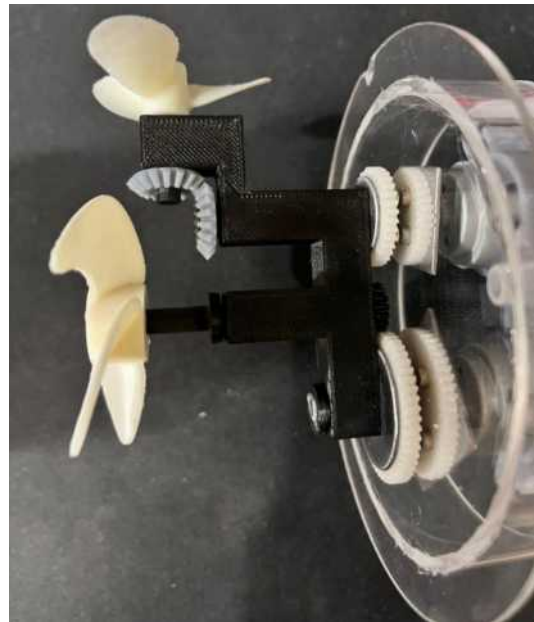
Figure 8: Two propellers.

3.1.4 Pressure Sensor

The pressure sensor chosen for integration into the project is the Honeywell SSCMANV030PA2A3, as depicted in Figure 9. This sensor employs the Inter-Integrated Circuit (I2C) communication protocol, a synchronous, multi-master, multi-slave, packet-switched, single-ended, serial computer bus. This protocol facilitates the transmission of data between the pressure sensor and the microcontroller, thereby enabling the accurate measurement and relay of pressure data. The use of the I2C communication protocol is

11

pivotal in ensuring the streamlined and efficient exchange of information, thereby contributing to the overall efficacy and functionality of the sensor within the operational parameters of the project.

Figure 9: Pressure Sensor.

Further technical specifications of the pressure sensor can be referenced in Figure 10 below, extracted from the datasheet in references. These specifications provide additional insights to assist in a comprehensive understanding of the sensor's capabilities and limitations. As previously discussed, the device operates on the principle of absolute pressure, measuring pressure relative to a vacuum, thereby negating the influence of surrounding ambient pressure fluctuations. Equipped with a barbed port, the sensor is well-suited for use in liquid media, offering a pressure range from 0 to 30 psi (2.06 bar). The sensor's absolute nature limits its effective range relative to atmospheric pressure to a maximum of 1 bar, corresponding to a depth measuring capacity of up to 10 meters—sufficient for the submarine's operational requirements. With a sample rate of up to 1000 samples per second and a 1 millisecond response time, the sensor delivers data with a 12-bit (0.03%) resolution, translating to an approximate depth measurement accuracy of 0.5 centimeters, a factor that warrants further assessment in relation to the project's specific needs.

Characteristic	Min.	Typ.	Max.	Unit
Supply voltage (V_{supply}):[1, 2, 3]				
pressure ranges ≥60 mbar | 6 kPa | 1 psi:				
3.3 Vdc	3.0	3.3	3.6	
5.0 Vdc	4.75	5.0	5.25	Vdc
pressure ranges ≤40 mbar | 4 kPa | 20 inH₂O:				
3.3 Vdc	3.27	3.3	3.33	
5.0 Vdc	4.95	5.0	5.05	
Supply current:				
3.3 Vdc	—	2.1	2.8	mA
5.0 Vdc	—	2.7	3.5	
Operating temperature range[4]	-40 [-40]	—	85 [185]	°C [°F]
Compensated temperature range[5]	-20 [-4]	—	85 [185]	°C [°F]
Startup time (power up to data ready)	—	—	5	ms
Response time	—	1	—	ms
Clipping limit:				
upper	—	—	97.5	%Vsupply
lower	2.5	—	—	
Accuracy[6]	—	—	±0.25	%FSS BFSL[8]
Output resolution	0.03	—	—	%FSS
Orientation sensitivity (±1 g):[7, 9]				
pressure ranges ≤40 mbar | 4 kPa | 20 inH₂O	—	±0.1	—	%FSS[8]
pressure ranges ≤2.5 mbar | 250 Pa | 1 inH₂O	—	±0.2	—	

Figure 10: Operating Specifications.

In consideration of ease in integration, the selected pressure sensor features a Surface Mount Technology (SMT) package, thus facilitating the soldering process. A visual representation of the sensor post-soldering can be observed in Figure 11, which depicts the incorporation of heat-shrink tubing and the attachment of a silicone hose to the port. This assembly not only ensures a secure and protected connection but also optimally positions the sensor for its intended underwater application.
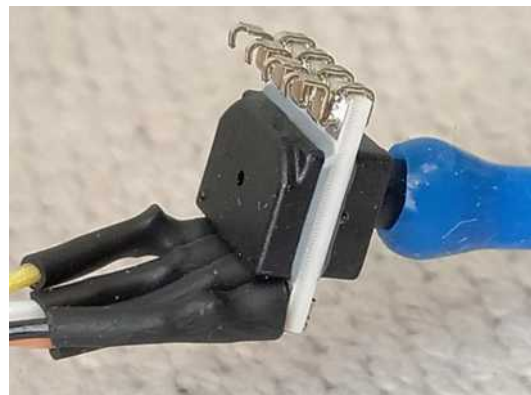

Figure 11: Pressure Sensor Wiring Connection.

13

3.1.5 Laser Distance Sensor

During the evaluation of the pressure sensor, contemplation arose regarding alternative methods of measuring underwater depth. One potential avenue explored was the utilization of sonar technology, which operates by reflecting sound waves off surfaces to ascertain distance. However, this pursuit was met with the challenge of sourcing cost-effective sonar components, with the available ultrasonic distance sensors proving to be potentially unsuitable due to their lack of compatibility with underwater conditions, uncertainty regarding their performance through hull walls, and questionable directionality.

Alternatively, laser distance sensors, which employ electromagnetic radiation akin to human vision, were identified as a potential solution. The premise relies on the transparency of water; should the water possess sufficient clarity, the laser sensor is anticipated to function effectively, mirroring the capabilities of the human eye in transparent media. Moreover, given that the submarine's hull is composed of transparent acrylic plastic, the laser sensor necessitates no waterproofing, as the laser can be transmitted directly through the hull walls. However, it is pertinent to note that measuring the water surface directly may not be feasible due to the reflective properties of water when a laser is projected perpendicularly. In such a case, measuring the distance to the lake's bottom may prove to be a more pragmatic approach, especially in scenarios involving proximity to the lakebed.

The chosen instrument for distance measurement in this project is, as in Figure 12 below, TF Mini LiDAR (ToF) Laser Range Sensor. This unidirectional laser range finder utilizes time-of-flight (ToF) technology, incorporating specialized optical and electronic devices, and an adaptive algorithm to cater to both indoor and outdoor environments. The TF Mini LiDAR is characterized by its compact size and high-performance capabilities in distance measurement.

Figure 12: Laser Distance Sensor.

The TF Mini LiDAR is equipped with a UART (TTL) communication interface and operates on a standard 5V supply, with an average power consumption of 0.6W. Furthermore, the sensor is compatible with various controllers and can be seamlessly integrated with Raspberry Pi 3A+, thereby facilitating direct plug-in capabilities, without the need for additional wiring. The connection is as in Figure 13 below:
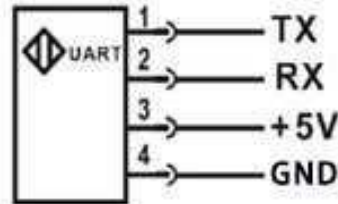
Figure 13: TF mini line sequence description.

3.1.6   Radio Frequency Controller

The submarine necessitates a radio controller operating at low frequencies, specifically within the 27 MHz, 40 MHz, and 75 MHz bands, to ensure effective penetration through water. Radio controllers operating within these frequencies are challenging to procure due to the prevalence of 2.4 GHz controllers in the market.

To circumvent this limitation, an alternative approach was adopted, involving the purchase of miniature toy submarines which are shown in Figure 14 below that operate at the desired frequencies. The components from these toys were then repurposed to serve the project's requirements. A mini toy submarine from Kogan was selected, meeting the project criteria with its utilization of a 27 MHz radio frequency.

Figure 14: Toy Submarine from Kogan.

The design aesthetic of the accompanying transmitter, although toy-like as in Figure 15, was visually appealing and fulfilled the desired functionality with its six-button control interface comprising left, right, forward, backward, dive, and surface.

Figure 15: Radio Transmitter (Controller).

Subsequent to verifying the operational functionality of the toy submarine, the process of disassembly was initiated. This entailed severing all connections to the motors and extracting the single printed circuit board housed within. The extracted board is presented in Figure 16 for reference.
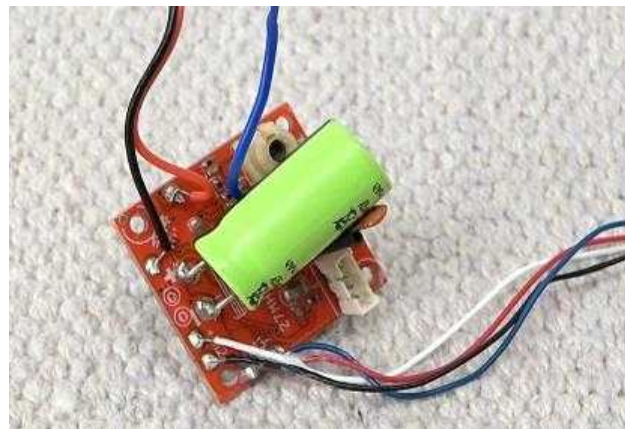
Figure 16 : Transmitter board from toy submarine

3.1.7 Mini Camera

The Camera Module 3 as in Figure 17 represents a significant enhancement in imaging capabilities, featuring a 12-megapixel sensor complemented by a high dynamic range mode and ultra-fast autofocus functionality. Furthermore, a comprehensive suite of software commands is available to facilitate precise control over the imaging process.

Figure 17: Raspberry Pi Camera Module 3.

Installation of the camera module is facilitated through the utilization of the included ribbon cable, which interfaces with the Camera Serial Interface (CSI) connector located adjacent to the HDMI ports on the Raspberry Pi. It can be referred to Figure 18 for visual guidance on the installation procedure.
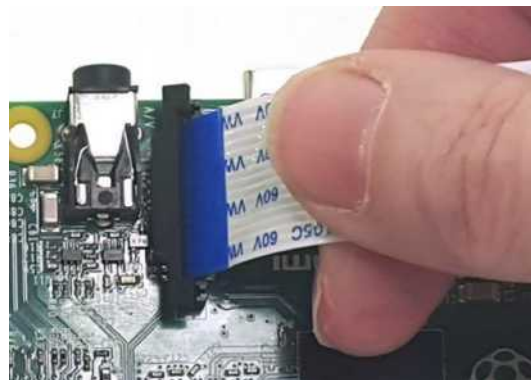
Figure 18: Installation on Raspberry Pi 3 Model A+.

It is crucial to note that the Camera Module 3 is not compatible with the legacy camera interface, necessitating the employment of 'Libcamera' commands. Consequently, the 'Raspistill' and 'Raspivid' commands, prevalent in previous iterations, are not applicable

to this module. Additionally, should the version of Raspberry Pi OS in use predate January 2023, a firmware update will be requisite to ensure compatibility with the new V3 camera.

3.1.8 Step Down Voltage Regulator

The acquired item, a BlueSky Universal Battery Eliminator Circuit (UBEC) 5V 3A DC-DC Converter Step Down Module as in Figure 19, functions as a voltage converter, designed to facilitate the derivation of a 5V output voltage from an input voltage range associated with 2-6S battery packs. This module is integral in ensuring a stable and regulated voltage supply for the electronic components of the system, thereby safeguarding them from potential voltage irregularities that may arise from the battery pack.

Figure 19: BlueSky UBEC 5V 3A DC-DC Converter Step Down Module.

3.1.9 Motor Driver

In order to facilitate the operation of DC motors, it is imperative to incorporate motor drivers, given that the Raspberry Pi is capable of supplying 5V and lacks the requisite current handling capability. These drivers must possess the capability to modulate both the speed and the direction of rotation of the motors. H-bridges are proficient in achieving this control when interfaced with Pulse Width Modulation (PWM) signals.

From empirical observations gathered during the utilization of submarine, it was deduced that the DRV8833 motor driver as depicted in Figure 20 exhibited an efficiency ranging from 70% to 90%.

Figure 20: Motor Driver.

3.1.10 DC Motor

The underwater submarine employs two direct current motors, specifically the RS PRO Geared motors in Figure 21 below, each with a power rating of 24.6 watts. These motors operate within a voltage range of 3 to 7.2 volts direct current, have a torque output of 107.3 gram-centimeters, and achieve a rotational speed of 22356 revolutions per minute. The shaft diameter of each motor measures 2.3 millimeters.

The first motor has been designated for facilitating the forward and backward locomotion of the submarine. By modulating the direction of the current, the submarine can be maneuvered in the desired orientation, thereby achieving longitudinal movement. The second motor, conversely, is tasked with imparting rotational motion to the submarine, thereby enabling it to execute turns to the left or right. This is achieved by altering the direction of the rotational force generated by the motor, which in turn, acts upon the propeller system to which it is connected. The implementation of these two motors, in conjunction with their associated propellers, forms the primary propulsion mechanism of the submarine, ensuring that it is well-equipped to navigate the aquatic environment in which it operates.

Figure 21: DC Motor.

3.1.11 Servo Motor

The ballast system of the underwater submarine incorporates the DF15RSMG 360-degree motor, a specific type of servo motor, to precisely control a syringe mechanism. This syringe functions as a crucial component in managing the intake and expulsion of water, thereby facilitating the regulation of the submarine's buoyancy.

The DF15RSMG 360-degree motor is known for its precise control capabilities, which allows for exact manipulation of the syringe plunger. In operation, the servo motor drives the plunger to create a vacuum effect within the syringe, leading to the ingress of water. This action incrementally adds to the submarine's weight, enabling controlled submersion and depth maintenance within aquatic environments.

By employing the DF15RSMG 360-degree motor, the submarine gains the advantage of finely tuned buoyancy management. This level of precision ensures that the submarine maintains stable and controllable operations in underwater environments, thereby enhancing the overall performance and effectiveness of the system. The overview of the servo motor can be seen in Figure 22 below.

Figure 22: Servo Motor.

3.1.12 Minicomputer

The Raspberry Pi 3 Model A+ as shown in Figure 23 was selected as the preferred computing module, boasting a 1.4GHz 64-bit quad-core processor and 512MB of LPDDR2 SDRAM. The performance offered by this module is deemed sufficient for the intended application. For storage, a 16GB microSD card was procured, ensuring ample space for the storage of generated log files. The compact form factor of the board, measuring 65×56 mm, renders it an apt choice for integration within the confined space of the submarine. The pinout diagram for the Raspberry Pi Model A+ can be referred to Appendix 1.

The inclusion of wireless LAN connectivity on the Raspberry Pi 3 Model A+ has proved invaluable, facilitating the implementation of code revisions remotely. This capability has significantly expedited the development process by obviating the need for physical access to the module for USB cable connections. The utility of wireless LAN in this context cannot be overstated, establishing it as a vital feature for efficient project development.

Figure 23: Raspberry Pi 3 Model A+.

Following the procurement of the Raspberry Pi 3 Model A+ and the 16GB microSD card, the subsequent step entailed the installation of the operating system onto the microSD card. The Raspberry Pi Foundation has conveniently provided a desktop imager program, which facilitates the process of installing an operating system onto the microSD card. Leveraging this utility, the Linux-based Raspberry Pi OS was selected and successfully installed onto the card.

Post-installation, the system was configured to enable Secure Shell (SSH) and Virtual Network Computing (VNC) protocols. This configuration allows for remote control and access of the Raspberry Pi from an external device, in this case, a laptop. For the execution of command-line operations and coding from the laptop, the software application PuTTY was utilized. PuTTY enables secure remote access to the Raspberry Pi using its IP address, thereby providing a convenient and efficient means of interfacing with the Raspberry Pi for the purpose of coding and other development activities.

For the execution of Python code, Thonny Python Integrated Development Environment (IDE) was employed, which is conveniently prepackaged with the Raspberry Pi OS. This software tool provides a user-friendly interface for the development and testing of Python scripts, thereby facilitating an efficient coding environment within the Raspberry Pi ecosystem.

3.2 Schematic Design

The core design ethos underpinning the underwater drone's development is anchored in a systematic and iterative engineering framework. This methodology accentuates modular principles, which bolster streamlined procedures during ensuing phases of upgrade, maintenance, and diagnostics, congruent with established engineering standards. Mechanical components within this initiative are conceptualized utilizing 3D CAD tools and materialized through additive manufacturing techniques. In contrast, the electrical and electronic schematic are designed using Autodesk EAGLE Software, as delineated in Figure 24. A comprehensive inventory of utilized components and materials is cataloged in Appendix 2.
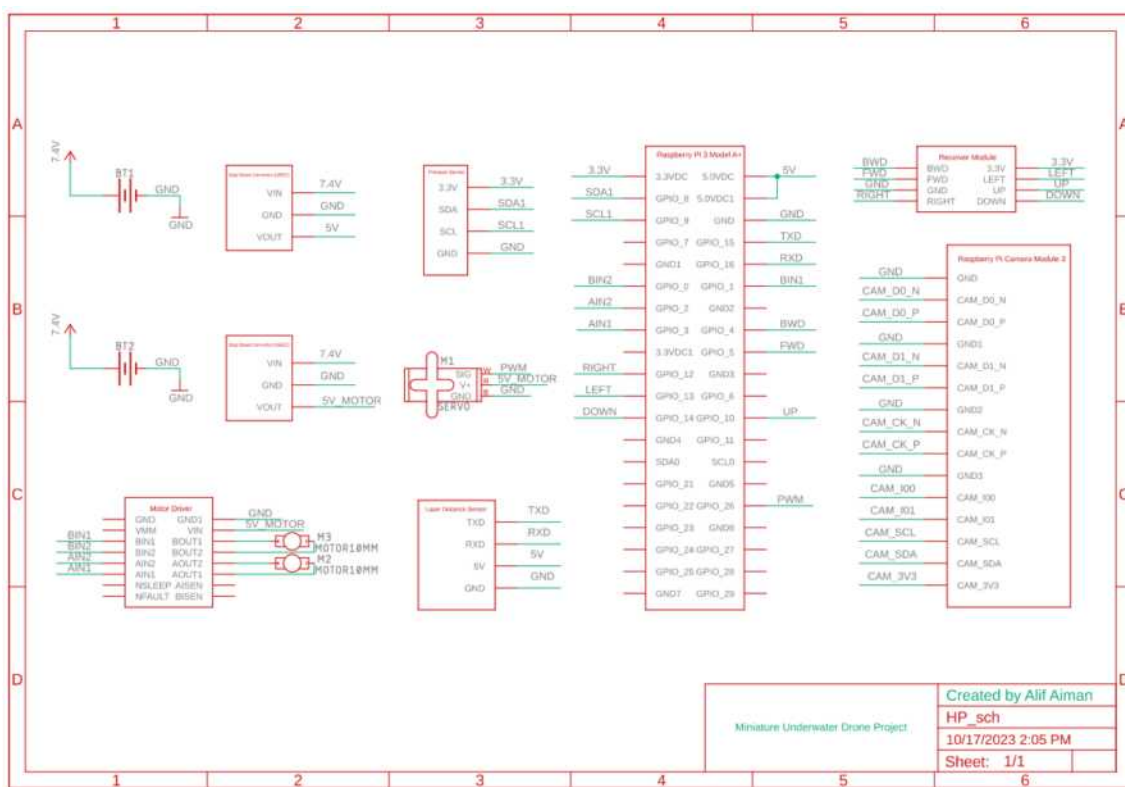
Figure 24: Schematic design for the project.

By referring to the schematic diagram presented in Figure 24, two independent 7.4V LiPo batteries, labeled as BT1 and BT2 on the schematic, serve as the foundational power sources for the entire system. Their primary role is to provide main power, which is subsequently conditioned to suit the needs of various components in the setup. Each of these 7.4V LiPo batteries is directly interfaced with a dedicated Step Down Converter Module. These converters play a pivotal role in regulating the supplied voltage, ensuring the downstream components receive a steady and safe power level.

The first Step Down Converter Module outputs a consistent 5 Volts (5V) voltage and 3 Amps (3A) current, specifically allocated for the Raspberry Pi 3 Model A+. This ensures that the central computing unit operates without interruptions, maintaining its critical functions throughout. Conversely, the second Step Down Converter Module, also standardized at a 5V output with 3A current, is dedicated to powering the servo (M1) and the two DC motors (M2 & M3). Ensuring a distinct and consistent power supply for these components is crucial, given their role in the drone's motion and maneuverability.

Beyond the servo and DC motors, the entire peripheral suite, comprising components like the Laser Distance Sensor and the Raspberry Pi Camera Module 3, directly derives its power from the Raspberry Pi 3 Model A+. This approach towards a centralized power distribution strategy not only optimizes energy management but also streamlines the overall system design by reducing the necessity for intricate power delivery networks.

Serving as the primary communication, the Raspberry Pi 3 Model A+ is integral for signal interactions between the system components. These communications predominantly occur via the Raspberry Pi's GPIO (General-Purpose Input/Output) pins. For instance, the Laser Distance Sensor establishes its connection to the Raspberry Pi through TxD (Transmit Data) and RxD (Receive Data) signal lines. Similarly, motor control signals originate from the Raspberry Pi and are routed to the Motor Driver, which then translates these signals into tangible actuations for the DC motors (M2 & M3). Furthermore, the Raspberry Pi Camera Module 3 interfaces with the Raspberry Pi to facilitate image and video processing, evident from the data signal exchanges, such as CAM_D0_N, CAM_D0_P, and others.

The inclusion of a pressure sensor in the drone's design is paramount for efficient underwater navigation. This sensor operates by continuously monitoring the ambient pressure, thus providing a reliable method to gauge the drone's depth. Its importance is underscored by the safety implications; by constantly assessing the operational depth, the drone can maintain set limits and avoid potential hazards.

From a communication perspective, the pressure sensor interfaces with the Raspberry Pi 3 Model A+ via the I2C (Inter-Integrated Circuit) protocol. I2C is a two-wire serial communication protocol that ensures synchronous data transmission between devices. In the context of the drone's design, the pressure sensor communicates using the SDA (Serial Data) and SCL (Serial Clock) lines. This setup enables bi-directional data transfer, allowing the Raspberry Pi to receive real-time pressure readings and, if required, send configuration or calibration commands to the sensor. The adoption of the I2C protocol ensures that communication is both swift and reliable, crucial for maintaining stable and controlled

underwater operations.

3.3 Mechanical Design and System Development Process

The mechanical components of the drone, encompassing both the hull and internal structures, were designed and constructed using the following methodologies:

The hull was fashioned from an acrylic cylinder, with both ends hermetically sealed using caps. These caps were constructed by adhering a 2 mm acrylic circular sheet to an acrylic tube boasting a thickness of 20 mm, an outer diameter of 100 mm, and an inner diameter of 95 mm. The rear cap, characterized by the location of the propellers, featured two 3.5mm diameter holes. These holes served dual purposes: one to interface a pressure sensor with the surrounding environment and the other to intake water into a syringe, essential for regulating the drone's diving mechanism. Additionally, to ensure a watertight seal between the cap and the cylindrical hull, two rubber O-rings were custom-made. This entailed aligning both ends of an O-ring cord, with specifications of 2.5 mm diameter and 250 mm length, against a 90-degree metal corner. A preliminary water test was conducted by filling the hull with water for several hours. Observations confirmed no leakage, minimizing the potential for electronic component damage due to water infiltration.

The rear cap also played a pivotal role in accommodating the transmission assembly, a system ingeniously designed to convey power from internal motors to external propellers via Neodymium magnets and an array of gears. To anchor these magnets to the gears, 1 mm thick steel boards were segmented into smaller units. Post segmentation, these units were adhered to the rear of the gears. Strategically, magnets were positioned on these steel units through gear-specific holes. Interestingly, magnets were oriented in pairs, with opposing poles facing in a uniform direction. The strong magnetic forces necessitated friction reduction. This was achieved by applying Ultra-High-Modular-Weight (UHMW) tapes at the cap-magnet interface. Research from curbellplastics.com [9] indicated a low friction coefficient of 0.1 for UHMW tapes, rendering them superior to most alternative materials. For propulsion purposes, propeller models were procured online. Post acquisition, each propeller was adapted with a 5 mm hole, ensuring compatibility with the designed transmission mechanism.

Internally, a semicircular structure complemented by a board was incorporated to anchor various components securely. Situated near the drone's rear, motors essential for propulsion and navigation were anchored. Centrally, a diving control system was integrated. Within this system, gears (each measuring 30 mm in diameter and having a module number of 1.25) facilitated power transfer from a servo motor to a strategically

placed syringe. This syringe, activated by the servo motor, modulated the drone's buoyancy by drawing in or expelling water. Additionally, counterweights were meticulously positioned at the hull's base to ensure the drone's equilibrium, thereby preventing inadvertent capsizing. All other electronic components found placement atop the board. The entire design and modeling process was built using CAD software and can be referred to Figure 25 below for the full 3D Design inside the drone.
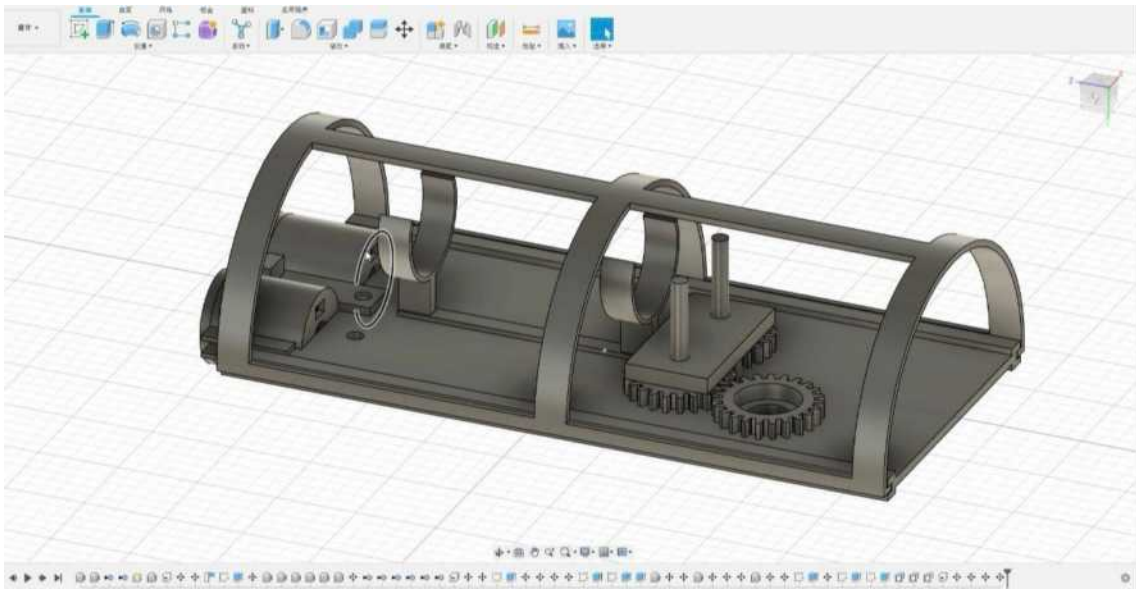
Figure 25: Full 3D design inside the drone.

3.4 Software Development Process

Crafting the software that drives the underwater drone necessitates an adaptive process, ensuring each software component aligns seamlessly with the drone's operational imperatives. This section illuminates the structured and evolutionary approach adopted in the software development journey. From the selection of methodologies that embrace change and flexibility to rigorous code assessments ensuring unerring execution, every phase is delineated with precision. Diving into this segment reveals the methodologies, practices, and tools employed to ensure that the software remains robust, adaptable, and primed to meet the multifaceted challenges of aquatic operations.

3.4.1 Code Testing

During the code testing phase, a systematic approach was employed to ensure each component functioned as intended. Initially, basic code was developed and implemented to individually test each component, verifying that all subsystems were operational. This process involved running separate test codes for each component to confirm their respective functionalities. Only after the successful validation of each component, were efforts directed towards the development of a comprehensive code. This comprehensive code aimed to harmonize all individual components, thereby ensuring seamless integration and optimal functioning of the overall system. This step-by-step approach facilitated a smooth transition from standalone subsystem testing to the realization of a fully integrated, cohesive system, aligned with the operational requirements of the drone.

3.4.2 Code Review and Quality Control

During the software development process, when errors or inconsistencies arose, a rigorous and systematic approach to problem-solving was employed. Initially, the issue was tackled utilizing a repertoire of programming knowledge and experience, carefully analyzing and troubleshooting the problem. This was particularly pertinent given the unique configurations and settings of the Raspbian Operating System, which serves as the bedrock of the drone's computational framework. It is essential to understand that errors might not necessarily stem from flaws within the code but could be a consequence of overlooked settings or misconfigurations within the operating system itself. An illustrative example of this is the Inter-Integrated Circuit (I2C) functionality. Failures in this realm could be attributed to neglecting to enable the necessary I2C settings, rather than any coding inconsistencies. If the issue remained unresolved following this initial phase of internal troubleshooting, the strategy shifted towards seeking external solutions and insights through in-depth internet research. This layered approach to problem-solving ensures a comprehensive and well-informed method, exploring all possible avenues before converging upon an optimal solution. It underscores the necessity of a deep and thorough understanding of the system's intricacies and configurations prior to resorting to external resources for the rectification of software anomalies.

3.5 Integration and Calibration

The journey from isolated components to a cohesive underwater drone system involves intricate steps of hardware with software, and finetuning them for optimal performance. This section delves into the processes of integrating diverse components into a unified operational framework and the subsequent calibration efforts undertaken to guarantee precision in the drone's readings and actions. It underscores the importance of creating a seamless interface between disparate elements, ensuring synchronized operations, and the criticality of validating each component's functionality against established standards. Readers will gain insights into the protocols, methodologies, and challenges encountered during these pivotal phases, underscoring the essence of integration and calibration in actualizing the drone's envisioned capabilities.

3.5.1 Hardware-Software Integration

The challenge of successfully integrating the Raspberry Pi with multiple sensors and actuators was anticipated from the project's outset. Each of these components, with distinct operational protocols and data communication standards, necessitated a well-strategized integration. To ensure streamlined communication between the hardware components and the core control software developed on the Raspbian Operating System using Python, specialized middleware scripts were designed. These scripts, functioning as the intermediate layer, decoded and translated data signals to and from the Raspberry Pi, providing a unified interface. Not only did this enable real-time data exchange, but it also ensured timely actuation commands were dispatched, resulting in synchronous and harmonious drone operations.

3.5.2 Calibration Procedures

Upon achieving successful integration, an imperative next step was the comprehensive calibration of each sensor and actuator. Calibration was essential to ascertain and rectify any discrepancies in the data readings and actuation responses. Focusing on the Honeywell pressure sensor: it was subjected to an extensive calibration regimen. Multiple test scenarios were simulated in controlled environments, where the sensor's data output was juxtaposed against predefined standard values. By applying statistical methodologies and leveraging Python's data analysis libraries, systematic error corrections were performed. Through iterative testing, any drifts or biases in the sensor readings were identified and rectified, assuring optimal accuracy in depth measurements during actual underwater missions.

3.6 Testing Protocols

Ensuring the underwater drone's operational excellence and reliability requires a series of systematic and rigorous tests. This section outlines the multifaceted testing strategies employed, spanning from controlled simulated environments to real-world aquatic deployments. By dissecting each testing phase, the discussion illuminates the significance of validating the drone's hardware components, software logic, and their combined functionalities. The intent behind each testing type, be it in a digital simulation, individual component validation, or actual field evaluations, underscores the comprehensive measures taken to ascertain the drone's efficacy and reliability. As readers progress through this section, they will gain a deep understanding of the lengths to which the engineering team went to ensure that the drone not only met but exceeded its defined performance benchmarks.

3.6.1 Leakage Test

The validation of the acrylic hull, serving as the structural exoskeleton for the submarine, was prioritized as a critical component of the testing phase. This precautionary measure was imperative to ensure the absence of any leaks within the hull that could potentially compromise the integrity of the internal components. The acrylic hull, devoid of any sensors, actuators, or software modules, was submerged in a pool and subjected to an extended test duration of one full day. This timeframe was deemed sufficient to thoroughly assess the hull's capability to withstand water ingress.

Upon completion of the 24-hour submersion test, evaluation was conducted to ascertain the presence or absence of any water within the hull. The objective was to guarantee that the structural integrity of the hull was unimpaired, thereby affirming its ability to provide a watertight enclosure for the various internal components of the submarine. Only after the hull had successfully passed this rigorous leakage test, were efforts directed towards the integration of the mechanical parts, sensors, and other electronic components. This systematic approach to testing and validation was instrumental in ensuring that each component remained uncompromised by potential water damage, thereby safeguarding the overall functionality and longevity of the submarine.

3.6.2 Field Testing

With the assurance from simulated and component-level tests, the drone was then introduced to real-world underwater environments. These field tests, orchestrated under expert supervision, were conducted across various water bodies including freshwater lakes, saline coastal regions, and deeper oceanic zones. During these tests, the drone's adaptability to dynamic aquatic conditions like fluctuating salinity, varying water temperatures, and unpredictable currents was assessed. Furthermore, the drone's communication capabilities, navigation accuracy, and endurance were gauged in these real-world conditions. The insights derived from these field evaluations provided a holistic view of the drone's performance. Any discrepancies observed were cataloged, analyzed, and subsequently addressed, ensuring the drone was finely tuned to meet its intended operational goals.

4 Theory

The triumphant realization of the underwater drone project is contingent upon a profound grasp of multiple intertwined theoretical frameworks encompassing the domains of electronics, mechanics, and software engineering. This section delves rigorously into these foundational principles, furnishing a comprehensive understanding of the drone's design rationale and operational capabilities.

4.1 Radio Frequency Communication

There are few types of radio frequency signals that can be used for underwater communication. These radio frequency signals are limited due to the high absorption and scattering RF waves in the water. In general, electromagnetic waves with higher frequencies such as used in Wi-Fi or Bluetooth are more severely attenuated in water. There are specific frequency bands that are commonly used for underwater communication. These frequencies fall within the very low frequency (VLF) and ultra-low frequency (ULF) ranges. VLF signals typically range from 3 kHz to 30 kHz, while ULF signals are even lower, ranging from 300 Hz to 3 kHz. VLF and ULF signals can travel longer distances through water compared to higher frequency RF signals. They are used for various underwater communication applications, such as submarine communication, underwater data transmission, and scientific research. Acoustic communication, using sound waves, is the most common method for long-range underwater communication, as sound waves can travel much farther in water than RF waves. Sonar systems, underwater acoustic modems, and underwater acoustic beacons are examples of technologies that utilize acoustic signals for underwater communication [2].

4.2 Underwater Acoustic Communications

Acoustic communication is widely used for underwater applications due to its ability to transmit over long distances. It involves sending and receiving sound signals through the water. Acoustic communication systems can be used to establish a communication link between the remote-controlled submarine. However, the data transfer rate for acoustic communication is relatively slow. The sound propagation of the acoustic communication travels differently in water compared to air due to differences in density and acoustic properties [4]. The speed of sound in water is much higher than in air, but it attenuates more rapidly over distance. Additionally, sound in water can be affected by factors like temperature, salinity, and depth. Underwater acoustic communication faces several challenges due to the characteristics of the underwater environment. These challenges include limited bandwidth, long propagation delays, signal attenuation, multipath interference, ambient noise, and Doppler shifts caused by the relative motion between the
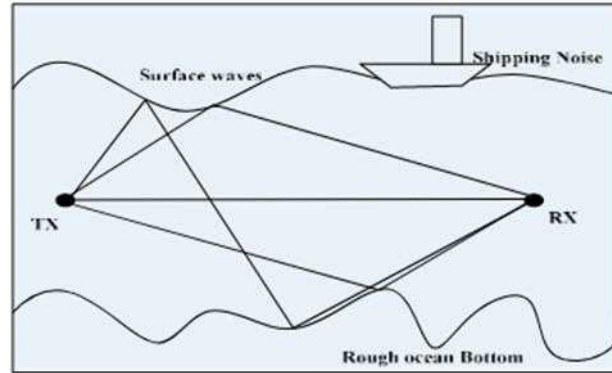
transmitter and receiver [5].

Figure 26: Underwater channel of multipath system [5]**.**

Figure 26 shows the one of the phenomena in underwater acoustic communication where sound waves traveling through water reach the receiver via multiple paths due to reflections, refractions, and scattering from various objects and boundaries in the underwater environment. Sound waves can bounce off the seafloor, surface waves, underwater structures, or any other objects present in the water. These reflections can result in multiple copies of the original signal reaching the receiver at different times. Sound waves can change direction as they pass through water layers with varying temperature, salinity, or pressure. These changes in direction can cause sound waves to propagate along different paths and arrive at the receiver with time delays. Sound waves can scatter off objects such as suspended particles, bubbles, and marine organisms. The scattered waves can interfere with the direct path signal, leading to variations in signal strength and arrival time at the receiver [5].

4.3 Thorpe's Formula for Transmission Loss

Transmission loss underwater is the depletion of strength of sound signals as it propagates through water. It occurs due to various properties that affect the transmission of sound waves in the underwater environment. Transmission loss in underwater RF communication is a critical consideration and is determined by factors like frequency, water temperature, salinity, and depth [3]. Thorpe's formula is a widely used model for estimating transmission loss [3]. It states that transmission loss (TL) in decibels (dB) can be calculated as follows:

$$TL = 20 \operatorname{Log}(r) + \frac{0.11\dfrac{f^2}{1+f^2} + 44\dfrac{f^2}{4100+f^2} + 2.75 \times 10^{-4}f^2 + 0.003}{1000}$$

Where r is the distance in meters, r is used to get the spherical spreading factor while f is

32

the frequency in kilohertz (kHz).

This formula illustrates the dependence of transmission loss on frequency, depth, temperature, and salinity, emphasizing the importance of selecting appropriate frequency bands for underwater RF communication [3].
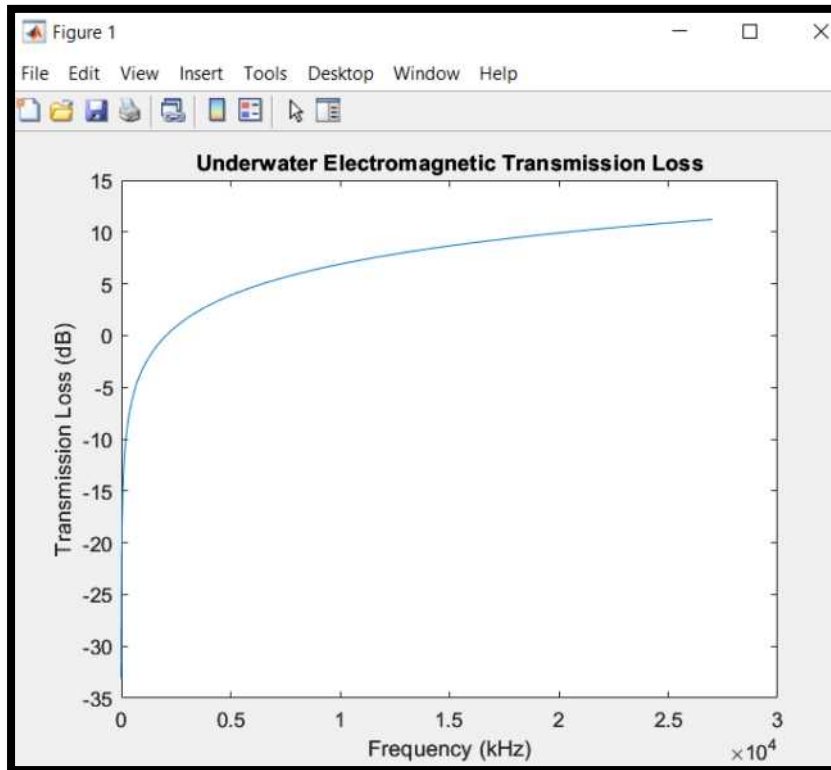

Figure 27: Transmission loss against frequency.

Figure 27 shows the result of transmission loss with different frequency underwater for 10-meter constant range based on the Thorp's equation. The x-axis of the plot represents the frequency in kilohertz (kHz), ranging from 1 kHz to 27 MHz. The y-axis represents the transmission loss in decibels (dB). Absorption coefficient increases as the frequency increases [3]. It is important to note that this simplified model may not capture all the complexities and variations of transmission loss in different underwater environments. Viscosity and ionic relaxation in water contribute to sound absorption. Viscosity primarily affects the medium frequency range [3]. Sound absorption is influenced by factors like frequency, salinity, temperature, pH, and depth [3].

4.4 Electrical and Electronic Component Theory

The main parts is the Raspberry Pi 3 A+, a robust and compact computational unit tasked with the responsibility of both controlling and processing all inbound and outbound signals. This unit's architecture boasts General-Purpose Input/Output (GPIO) pins, facilitating the seamless integration of a diverse range of sensors and modules. Distinct from conventional computer systems, the Raspberry Pi's streamlined design coupled with its expansive GPIO functionalities render it particularly suitable for embedded system applications. A thorough exploration of its operational capabilities and features is delineated in the official Raspberry Pi documentation, to which a link is provided.

The nuanced movement dynamics of the drone are intricately bound to Motor Control mechanisms and Pulse Width Modulation techniques. At its core, Pulse Width Modulation serves as a strategy to generate analog signals from a digital origin. This technique is fundamental in governing the speed and directional attributes of both servo and direct current motors. By modulating the duration of the active high state within each pulse cycle, one can achieve precise command over the motor's angular disposition or velocity, thereby bestowing refined control upon the drone's navigational trajectory.

The drone's wireless communication framework harnesses the capabilities of Radio Frequency communication. While Radio Frequency modalities are commonplace in terrestrial settings, their deployment underwater introduces distinct challenges, most notably signal attenuation. For operations confined to shorter spatial extents, Radio Frequency modules adapted from miniature submarine toys present an efficacious solution, underscoring the adaptability of Radio Frequency paradigms beyond conventional domains.

Ensuring the energetic demands of these electronic constituents is the Lithium Polymer battery, selected for its superior energy density and its capacity for recharging. Such batteries adeptly meet the elevated energy requisites of the drone, guaranteeing unwavering performance even during extended mission durations.

4.5   Mechanical Theory

The core of the drone's aquatic navigational capabilities is the principle of Buoyancy Control. Buoyancy is the determining factor dictating whether an object remains afloat or submerges within a fluid medium. This phenomenon is underscored by Archimedes' principle, which asserts that the upward buoyant force exerted on a submerged object is directly proportional to the weight of the fluid it displaces. By utilizing a servo motor to regulate a ballast tank, the drone is equipped to dynamically modulate its buoyancy, thereby achieving precise depth regulation.

Navigation within the aquatic milieu necessitates a comprehensive grasp of Fluid Dynamics. As the drone propels itself through water, it invariably confronts forces of drag and lift. A holistic comprehension of these forces is indispensable for optimizing its maneuverability. Additionally, the pressure exerted by the surrounding water intensifies proportionally with increased depth, posing challenges to both the drone's structural resilience and its movement parameters.

Instrumental in discerning these pressure variations is the Honeywell pressure sensor, which operates on the principle of piezo resistance. When the sensor is subjected to differential pressure, it undergoes a corresponding shift in its resistive value. This alteration is subsequently transduced into an electrical signal. Upon processing by the Raspberry Pi, this signal yields invaluable data regarding the drone's prevailing depth within the aquatic environment.

When designing 3D printing models, since the models are printed at 200 degrees Celsius, the model will shrink after it is cooled down to room temperature. According to Filament2print [10], the shrinkage will be from 0.2% to 4% depending on the material used. Thus, to fit the parts into holes, the diameter of the hole should be around 104% of the shaft, and if the shaft is expected to rotate smoothly and stably inside the hole, the diameter should be 108%.

5 Results and Discussion

This section presents an in-depth exploration of the technical underpinnings of our underwater drone project. The intricacies of both hardware and software are dissected, from individual component functionalities to comprehensive system integrations. Additionally, this chapter will delve into the tangible outcomes achieved during the project's lifecycle and a critical discussion of these results in relation to our initial objectives.

5.1 Raspberry Pi 3 A+ and Camera Module

In the conducted tests, the Raspberry Pi exhibited exemplary performance, highlighting the advantages of integrating such robust computational units within aquatic drones. The Camera Module's capabilities were specifically evaluated in the controlled environment of a swimming pool with clear water conditions. Under these circumstances, the captured images showcased remarkable clarity and resolution, demonstrating the Camera Module's potential in environments with minimal water turbidity. However, there is a consideration to be made regarding its performance in natural water bodies with varying levels of turbidity. This observation underscores the importance of further testing in varied conditions to ensure consistent performance across different scenarios. Future iterations might explore enhancements or the integration of alternative imaging solutions to address challenges presented by turbid waters. The images taken during the test, as displayed in Figure 28, provide a visual representation of the results obtained in the swimming pool.
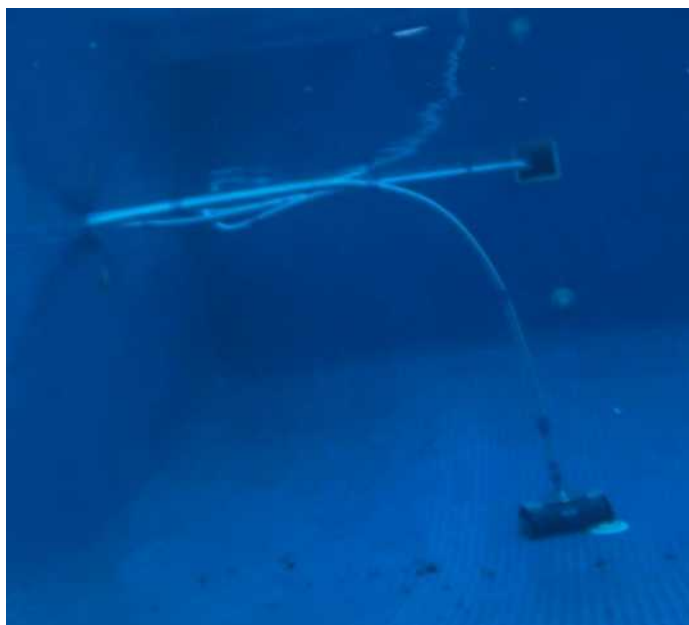

Figure 28: Images captured by the Raspberry Pi camera under clear water.

The drone's enhanced capabilities are further highlighted by the integration of real-time video streaming. Through the Raspberry Pi's "libcamera" function, the drone transmits live video feeds, granting operators a comprehensive view of the drone's immediate environment. Such a feature becomes invaluable, particularly when navigating intricate or unfamiliar terrains, as it permits remote monitoring and more informed decision-making.

The streaming process relies on the Transmission Control Protocol (TCP), a robust communications protocol essential for transmitting messages between application programs and various computational devices. TCP ensures the accurate and timely delivery of data across internet frameworks, bolstering the reliability of the drone's communication system. Given TCP's dependability, it serves as the foundation for numerous high-level protocols, especially those necessitating consistent and reliable data transmission. Prominent protocols such as File Transfer Protocol (FTP), Secure Shell (SSH), and Telnet are just a few examples that leverage TCP [11]. For this specific project, the SSH protocol becomes pivotal, offering secure communication channels with the drone.

Figure 29 offers a clear illustration of the system in action. Displayed on a laptop screen is the video feed, captured by the drone's camera and streamed using the 'libcamera' function. The command **'libcamera-vid -t 0 --inline --listen -o tcp://0.0.0.0:8554'** ensures continuous video streaming, while other devices on the same network can access this feed via VLC by opting for the Open Network Stream option and inputting **'tcp/h264://[IP_ADDRESS]:8554'**. It is pertinent to note that the IP address is dynamic, adjusting based on the specific network settings.

This capability, as evidenced by the figure below, fortifies the drone's functionality, allowing for real-time interventions, adjustments, and commands, reinforcing the significance of advanced communication tools in drone operations.
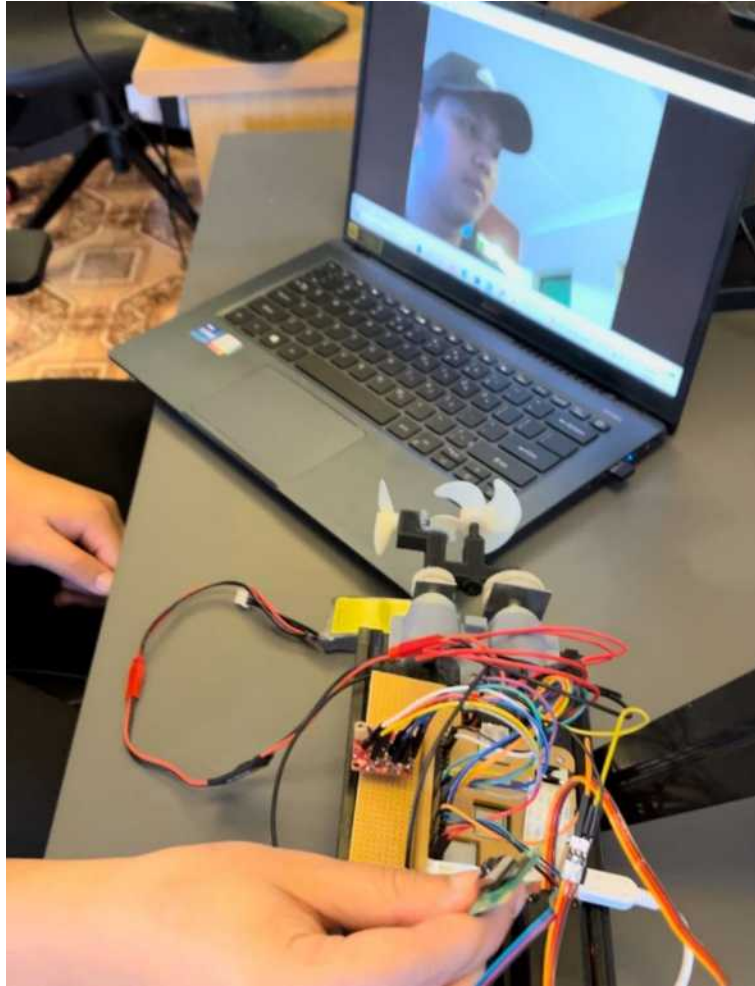
Figure 29: Live video stream through TCP.

5.2 Propulsion System

During evaluations of the propulsion system, distinct performance variations were observed between tests conducted outside the swimming pool and those within the aquatic environment. Outside the swimming pool, the propulsion system showcased a rapid motor speed. However, when subjected to the conditions within the swimming pool, a noticeable reduction in the motor's speed was evident, suggesting an increased load or resistance encountered by the motor while operating submerged in water. This variation underscores the impact of aquatic environments on motor performance, likely attributed to water resistance and the subsequent increase in drag. Such observations hint at potential areas of optimization for the propulsion system. Addressing these discrepancies might involve refining motor response algorithms, exploring advanced motor designs, or even reconsidering the overall design and material choices for the drone's external components to ensure consistent and optimal performance in varied water conditions.

5.3   Buoyancy and Depth Control

The initial evaluations of the buoyancy system revealed certain challenges in maintaining the desired depth, particularly during rapid transitions. One specific observation was a misalignment issue with the servo motor's rotation. During the preliminary test phase, a limit had not been set for the servo motor's rotation range. Consequently, the syringe, a critical component of the buoyancy system, made an uncontrolled motion until it reached its end point. While this action did not result in any broken teeth in the mechanical setup, it did lead to the gears slipping from their designated positions on the gear rack. Such displacement required reinstallation of the gears to restore the system's functionality.

To address this oversight, subsequent modifications were implemented in the system's control algorithm. A timer was introduced to limit the rotation duration of the servo motor, thereby ensuring that the syringe operated within its safe and intended range. With this corrective action in place, the buoyancy and depth control system exhibited enhanced performance, with precise depth transitions and increased reliability. However, the observed 5% variance in depth position still suggests the potential for further optimization, particularly in refining the system's feedback mechanisms by using tachometer.

5.4   Sensory Systems

The drone incorporates two fundamental sensory components: the TF Mini LiDAR for navigation and the Honeywell pressure sensor for depth measurement. The LiDAR stands out as an essential mechanism for obstacle detection, ensuring that the drone can navigate its surroundings without the risk of collisions. It communicates using the 'Universal Asynchronous Receiver / Transmitter' (UART) interface, employing TxD (Transmit Data), RxD (Receive Data) signal lines, and a grounding reference to guarantee accurate and timely data exchanges.

Simultaneously, the Honeywell pressure sensor provides crucial insights into the drone's depth within the water. Being able to gauge the drone's depth is indispensable for ensuring it operates safely and within set parameters. This pressure sensor utilizes the Inter-Integrated Circuit (I2C) protocol, employing the SDA (Serial Data) and SCL (Serial Clock) lines to facilitate the accurate transfer of depth information.

As showcased in Figure 30, the LiDAR system outputs a consistent set of readings pertaining to distance and signal strength. These readings, which vary between 4 cm and 6 cm and display different signal strengths, highlight the reliability and efficiency of the sensory system. Such data proves invaluable during the drone's operations, offering immediate insights into its proximity to nearby obstacles and prompting necessary navigational

corrections. The signal strength readings further illuminate the sensor's performance under varied operational conditions.

The Honeywell pressure sensor's depth readings further enhance the operational safety and accuracy of the drone. By continuously monitoring the depth, the drone can ensure it remains within prescribed operational boundaries, avoiding potential hazards and ensuring optimal performance.

In conclusion, integrating these sensory systems and evaluating their real-time readings accentuates the importance of continuous data monitoring in the drone's functions. The data obtained also emphasizes the potential for further refinements to optimize performance across different aquatic settings.


```
Distance: 6 cm, Signal Strength: 6939
Distance: 6 cm, Signal Strength: 6855
Distance: 6 cm, Signal Strength: 6694
Distance: 6 cm, Signal Strength: 6488
Distance: 5 cm, Signal Strength: 6275
Distance: 5 cm, Signal Strength: 6109
Distance: 5 cm, Signal Strength: 6005
Distance: 5 cm, Signal Strength: 5935
Distance: 5 cm, Signal Strength: 5832
Distance: 5 cm, Signal Strength: 5697
Distance: 5 cm, Signal Strength: 5586
Distance: 5 cm, Signal Strength: 5503
Distance: 4 cm, Signal Strength: 5452
Distance: 4 cm, Signal Strength: 5435
Distance: 4 cm, Signal Strength: 5418
Distance: 5 cm, Signal Strength: 5406
Distance: 5 cm, Signal Strength: 5389
Distance: 5 cm, Signal Strength: 5355
Distance: 5 cm, Signal Strength: 5344
Distance: 5 cm, Signal Strength: 5321
Distance: 5 cm, Signal Strength: 5302
Distance: 5 cm, Signal Strength: 5275
Distance: 5 cm, Signal Strength: 5269
Distance: 6 cm, Signal Strength: 5270
```

Figure 30: Output readings from the TF Mini LiDAR sensor in clear water.

5.5   Communication Systems

In aquatic environments, effective communication remains paramount to ensure real-time control and accurate data transmission. For this project, RF Communication was employed to steer the drone's movements. An RF Controller and an RF Receiver Board, disassembled from a toy submarine operating at a frequency of 27 MHz, were integrated to address the unique challenges of underwater communication. This system boasts 6 channels, which facilitate various maneuvers, including forward and backward motions, left and right turns, and diving and surfacing operations.

Further to the core system, the drone also incorporated a WLAN system, operating at a frequency of 2.4GHz. While this frequency has known limitations in water penetration, testing indicated a penetration depth of approximately 0.1-0.2 m. This range is just sufficient for communication when the drone is near the water's surface, an essential feature for system adjustments and software operations without having to extract the drone from water.

In controlled conditions within a big water container, the WLAN connection remained steady, allowing real-time console reading via a VNC connection—an essential feature for real-time troubleshooting.

However, tests in a swimming pool identified a consistent depth limitation of about 0.1m for the 2.4GHz frequency. The RF communication system's range was further scrutinized. Inside the drone's hull, with all components operational, the radio range was found to be around 3 meters. This was unexpected, as pre-assembly tests indicated a range of 7 meters. Attempts to augment this range with a longer antenna, based on past successes, unfortunately, yielded no improvements. The range remained within 3-4 meters.

Collectively, these results emphasize the importance of ongoing research and optimization in the design of underwater communication systems to ensure enhanced and consistent performance.

6 Recommendations for future work

Following an extensive analysis of performance metrics, technical considerations, and user feedback, this chapter outlines a comprehensive set of recommendations for subsequent drone iterations. These proposals aim to augment the underwater drone's efficacy, adaptability, and long-term performance.

6.1 Enhanced Propulsion System

The propulsion dynamics presently rely on conventional dual direct current (DC) motors. Exploring the realm of brushless motors might offer significant advantages. These motors, devoid of brushes, exhibit superior electromechanical efficiency, a noticeable reduction in maintenance needs, and an impressive torque-to-weight ratio. Transitioning to brushless motors could lead to extended operational times, fewer maintenance requirements, and enhanced maneuverability in complex underwater environments.

6.2 Improved Communication Systems

The existing Radio Frequency (RF) communication system, although functional, demonstrates certain limitations in challenging aquatic environments, especially in deeper or sediment-rich waters. Integrating acoustic modems, which utilize the principles of underwater sound wave propagation, offers a potential avenue for improving communication reliability. This innovative medium can ensure consistent data transmission and crystal-clear control signals even in conditions marked by high turbidity or profound depths.

6.3 Expansion of Sensory Capabilities

Elevating marine data collection capabilities necessitates the incorporation of a broader spectrum of sophisticated sensors. Consider the inclusion of high-precision temperature probes, advanced salinity meters to measure water's salt concentration accurately, and pH meters for real-time acidity or alkalinity monitoring. Equipping the drone with such a diverse array of sensors transforms it into a comprehensive marine research tool, primed for real-time data acquisition.

6.4 Machine Learning & AI Algorithms

Embedding advanced machine learning and artificial intelligence frameworks into the drone's architecture can revolutionize its capabilities. Leveraging algorithms that process and analyze voluminous sensory data will enable the drone to autonomously navigate challenging terrains, recognize marine objects, and even preemptively flag maintenance needs. Such integrations promise not only to enhance drone efficiency but also to minimize

manual oversight.

6.5 Reassessment of Structural Components and Materials

As the drone descends into the aquatic abyss, it confronts rising hydrostatic pressures. A comprehensive reevaluation of its construction materials becomes indispensable. Exploring materials like carbon fiber composites or specialized marine-grade polymers could offer superior strength while possibly reducing the drone's mass. This dual advantage can be instrumental in optimizing buoyancy and enduring greater depths.

6.6 Emphasis on Modular Architectural Design

Embracing a modular design philosophy for upcoming drone versions promises unparalleled versatility. This design approach facilitates effortless component swaps, allowing operators to modify the drone's hardware layout to fit distinct mission requirements. This flexibility in changing optical components, adjusting propulsion mechanisms, or adding specific research tools ensures that the drone remains adaptive to diverse operational scenarios.

6.7 Exploration of Renewable Energy Integrations

In line with global sustainability imperatives, it is prudent to investigate the integration of green energy solutions like miniature underwater turbines or cutting-edge photovoltaic modules. These renewable sources could supplement the primary power source, extending the operational longevity of the LiPo battery or even introducing self-recharging mechanisms.

6.8 Advancements in User Interactivity and Command Systems

Revolutionizing the control experience requires a transformative approach in user interface design. Delving into Virtual Reality (VR) or Augmented Reality (AR) technologies can provide operators with an enveloping, three-dimensional command ecosystem. Such interfaces, integrated with instantaneous data visualization techniques, can exponentially improve operators' situational awareness, precision in navigation, and overall mission efficacy.

7 Conclusion

In underwater exploration, the design and development of efficient and reliable drones stands as a testament to the convergence of cutting-edge technology and innovative engineering solutions. The comprehensive evaluation presented in this document touches upon the multifaceted elements involved in the realization of a successful aquatic drone.

Chapter 1 established a solid foundation by laying out the background, motivation, and primary aims of the project. It emphasized the significance of defining clear objectives and provided a broad overview of the document's structure. This initial insight was essential in setting the stage for the subsequent discussions and assessments. The Literature Review in Chapter 2 offered an in-depth analysis of existing technologies in the realm of Autonomous Underwater Vehicles (AUVs) and Remotely Operated Vehicles (ROVs). Such a review was imperative to discern the prevailing trends and identify potential areas of improvement.

Chapter 3, centered around Methodology, dissected the hardware components and system development processes. It provided a structured approach to the schematic design, mechanical design, software development, and the subsequent integration and calibration stages. The emphasis on testing protocols indicated the importance of rigorous validation in ensuring the reliability and efficiency of the system. The theoretical underpinnings, elaborated in Chapter 4, offered a detailed understanding of the various principles guiding the project. From radio frequency communication to mechanical theories, each section contributed to a deeper appreciation of the complexities involved in underwater drone development.

In Chapter 5, the discussion shifted to the results derived from the extensive tests and evaluations. These findings provided valuable insights into the operational capabilities of systems like the Raspberry Pi 3 A+, propulsion mechanisms, sensory systems, and communication frameworks. Chapter 6, focusing on Recommendations for Future Work, highlighted avenues for further research and development. The suggestions ranged from propulsion enhancements to the integration of Machine Learning & AI algorithms, underscoring the vast potential for future innovations in this domain.

In summation, the journey from conceptualization to realization of the underwater drone, as detailed in this document, showcases the immense potential that resides in the confluence of technology, engineering, and innovative thinking. It is hoped that this work will not only serve as a valuable reference but also inspire future endeavors in the field of underwater exploration and beyond.

8 References

[1] BrickExperimentChannel et al., "RC submarine 4.0 – background (1/10)," Brick Experiment Channel, Jun. 25, 2022. [Online]. Available: https://brickexperimentchannel.wordpress.com/2022/06/25/rc-submarine-4-0-background-1-10/. (Accessed: May 18, 2023).

[2] J. Lloret, S. Sendra, M. Ardid, and J. J. P. C. Rodrigues, "Underwater Wireless Sensor Communications in the 2.4 GHz ISM Frequency Band," Sensors, vol. 12, no. 4, pp. 4237-4264, Mar. 2012. doi: 10.3390/s120404237.

[3] S. Aydin and T. O. Onur, "Investigation of parameters affecting underwater communication channel," Journal of Engineering Sciences, vol. 7, no. 1, pp. F39-E44, 2020. doi: 10.21272/jes.2020.7(1).f4.

[4] S. Jiang and S. Georgakopoulos, "Electromagnetic Wave Propagation into Fresh Water," Journal of Electromagnetic Analysis and Applications, vol. 3, no. 7, pp. 261-266, 2011. doi: 10.4236/jemaa.2011.37042.

[5] B. Pranitha and L. Anjaneyulu, "Analysis of Underwater Acoustic Communication System Using Equalization Technique for ISI Reduction," Procedia Computer Science, vol. 167, pp. 1128-1138, 2020. doi: 10.1016/j.procs.2020.03.415

[6] R. B. Wynn et al., "Autonomous Underwater Vehicles (AUVs): Their past, present and future contributions to the advancement of marine geoscience," Marine Geology, vol. 352, pp. 451–468, Jun. 2014, doi: https://doi.org/10.1016/j.margeo.2014.03.012.

[7] F. Campagnaro, A. Signori, and M. Zorzi, "Wireless Remote Control for Underwater Vehicles," Journal of Marine Science and Engineering, vol. 8, no. 10, p. 736, Oct. 2020, doi: https://doi.org/10.3390/jmse8100736.

[8] Engineers Edge, "Densities of Metals and Elements Table," Engineersedge.com, Mar. 30, 2017. [Online]. Available: https://www.engineersedge.com/materials/densities_of_metals_and_elements_table_13976.htm. (Accessed: 15 Oct. 2023).

[9] Anonymous, "Plastic Material Properties Table | Sort & Compare," Curbell Plastics. [Online]. Available: https://www.curbellplastics.com/resource-library/material-selection-tools/plastic-properties-table. (Accessed: 10 Oct. 2023).

[10] Anonymous, "Shrinkage of parts in 3D printing and Warping," filament2print.com. [Online]. Available: https://filament2print.com/gb/blog/136_warping-contractions-3D-printing-parts.html. (Accessed: 11 Oct. 2023).

[11] Fortinet, "What is TCP/IP and How does it work?," *Fortinet*, 2021. [Online]. Available: https://www.fortinet.com/resources/cyberglossary/tcp-ip. (Accessed: 8 Oct.2023).

[12] Raspberry Pi Foundation, "Raspberry Pi Model 3A+ Product Brief," Raspberry Pi 3A+, Nov. 2018 [Accessed: Oct. 2023].

[13] Honeywell, "TruStability Board Mount Pressure Sensors," Single axial barbed port datasheet, [Accessed: Oct. 2023].

[14] Benewake, "TFmini Infrared Module specification," SJ-GU-TFmini-01, [Accessed: Oct. 2023].

[15] DFROBOT, "360 Degree Motor," DF15RSMG, [Accessed: Oct. 2023].

[16] RS Pro, "DC Motors," RS PRO DC Motor, 24.6 W, 3 to 7.2 V dc, 107.3 gcm, 22356 rpm, 2.3mm Shaft Diameter, [Accessed: Oct. 2023].

[17] Texas Instruments, "Dual H-Bridge Motor Driver," DRV8833 datasheet, January 2011 [Revised July 2015]

[18] Raspberry Pi Foundation, "Raspberry Pi Camera Module 3 Product Brief," Raspberry Pi Camera Module 3, Jan. 2023 [Accessed: Oct. 2023].

[19] Adafruit, "UBEC DC/DC Step-Down (Buck) Converter," 5V @ 3A Output datasheet, [Accessed: Oct. 2023].

9 Appendices

Appendix 1: GPIO (general-purpose input/output) pins for Raspberry Pi 3A+
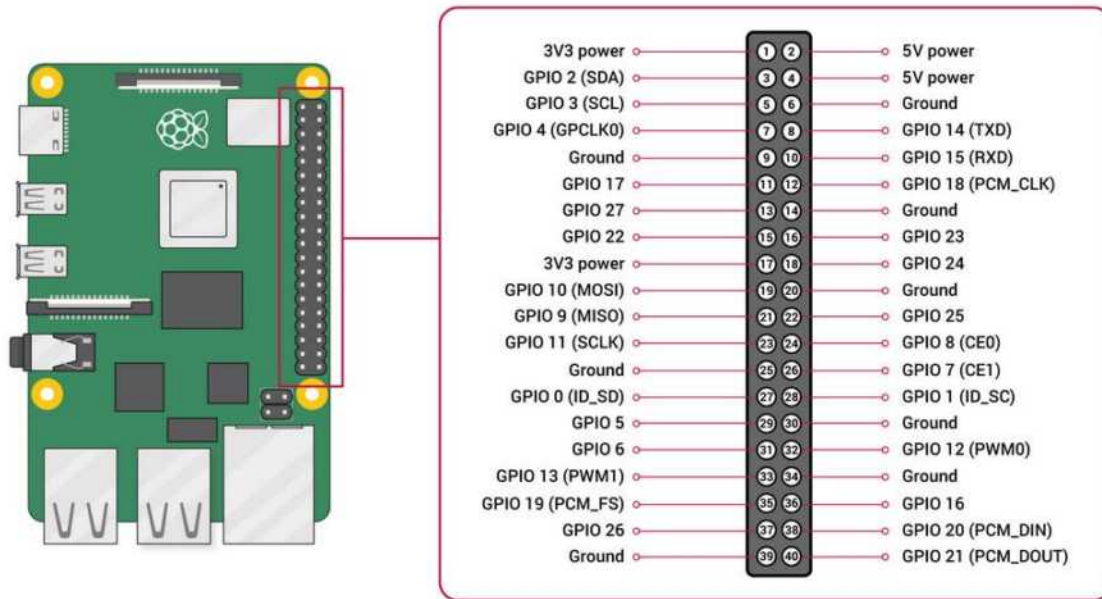
Appendix 2: Detail of components and items used in the project.

No.	Name	Description	Cost excluding delivery in AUD (Quantity)
1.	Single-Board Computer	Raspberry Pi 3 Model A+	$55.00 (1)
2.	Pressure Sensor	Honeywell Piezoresistive Pressure Sensor	$74.12 (1)
3.	Laser Distance Sensor	TF Mini LiDAR (ToF)	$71.20 (1)
4.	Li-Po Battery	1000mAh 7.4v 2S Battery Pack with JST Connector	$39.90 (2)
5.	Servo Motor	DF15RSMG 360 Degree Motor	$34.40 (1)
6.	DC motor	RS PRO Geared, 24.6 W, 3	$10.00 (2)

		to 7.2 V dc, 107.3 gcm, 22356 rpm, 2.3mm Shaft Diameter	
7.	Motor Driver	DRV8833 Dual Motor Driver Carrier (1.2A and low voltage)	$14.95 (1)
8.	Mini Camera	Raspberry Pi Camera Module 3	$48.50 (1)
9.	Step Down Voltage Regulator	BlueSky UBEC 5V 3A DC-DC Converter Step Down Module	$15.90 (2)
10.	Receiver Module	27 MHz controller dissembled from a toy submarine	$41.50 (1)
11.	Clear Acrylic	Clear tube and cap for the drone	Cap - $26.59 (2) Tube - $79.98 (1)
12.	Magnets	Used for magnetic coupling	$30.13 (1 set)
13.	O-ring	Prevent from leakage	$6.34 (1 metre)

Appendix 3: Drawings of 3D printed components used in the project.
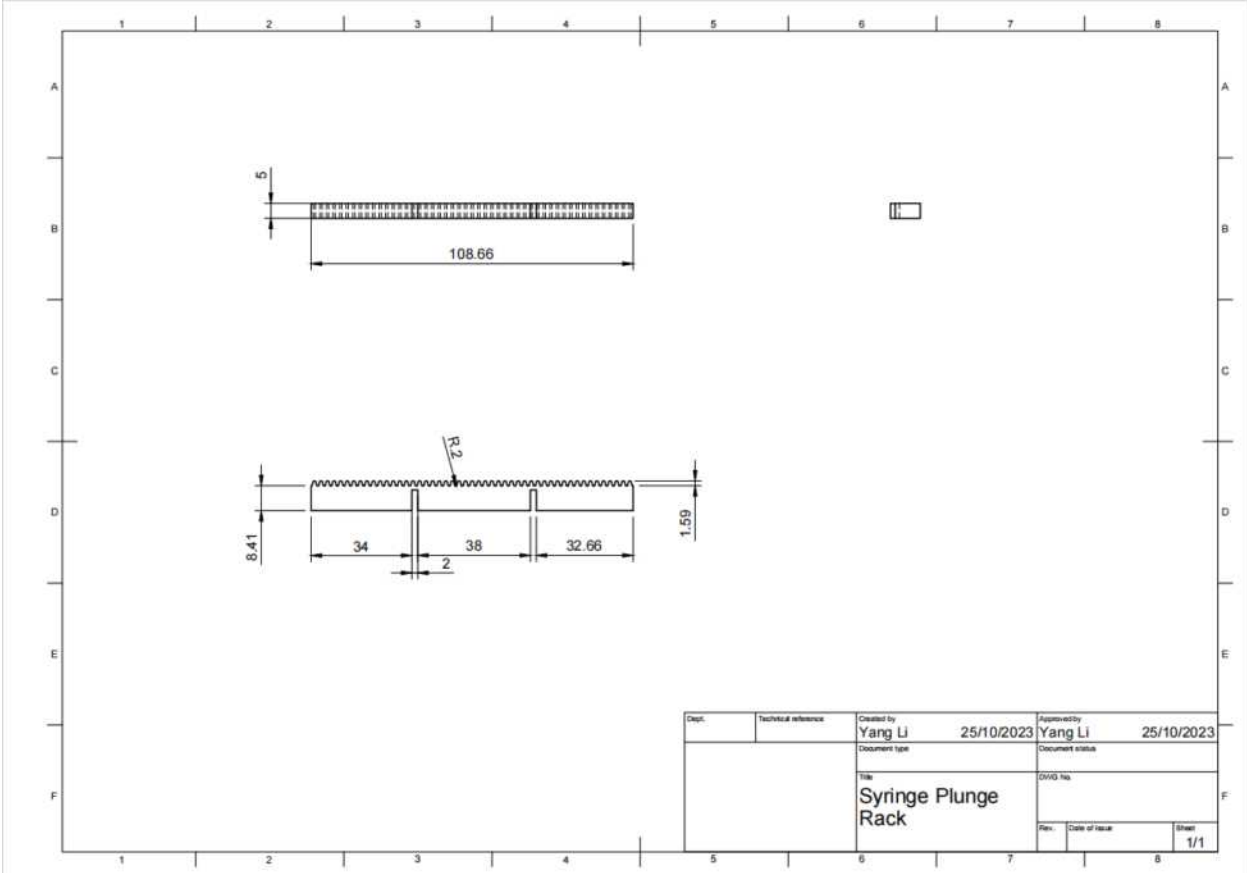
Figure 31: The rack glued on the syringe.
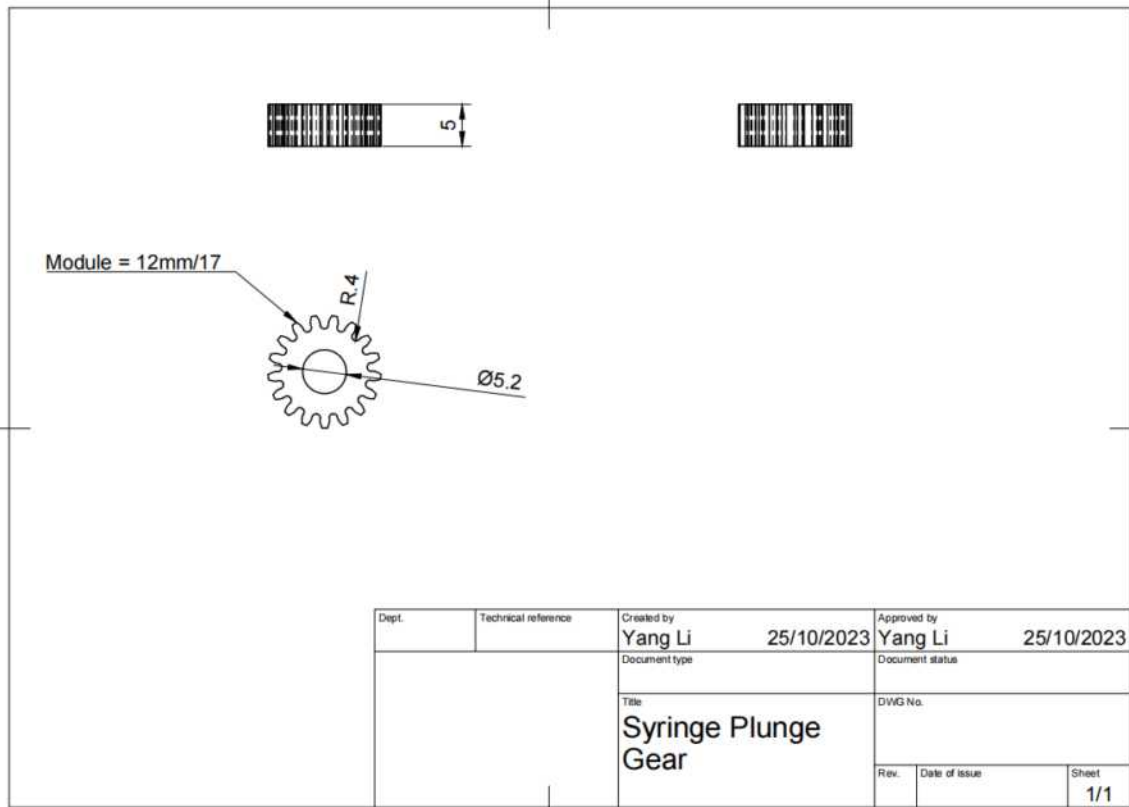
Figure 32: The Gear to drive syringe plunge.

Module = 30mm/23

R.2

Ø5.2

5

Dept.	Technical reference	Created by		Approved by	
		Yang Li	25/10/2023	Yang Li	25/10/2023
		Document type		Document status	
		Title		DWG No.	
		Syringe Transmission Gear			
				Rev.	Date of issue	Sheet 1/1
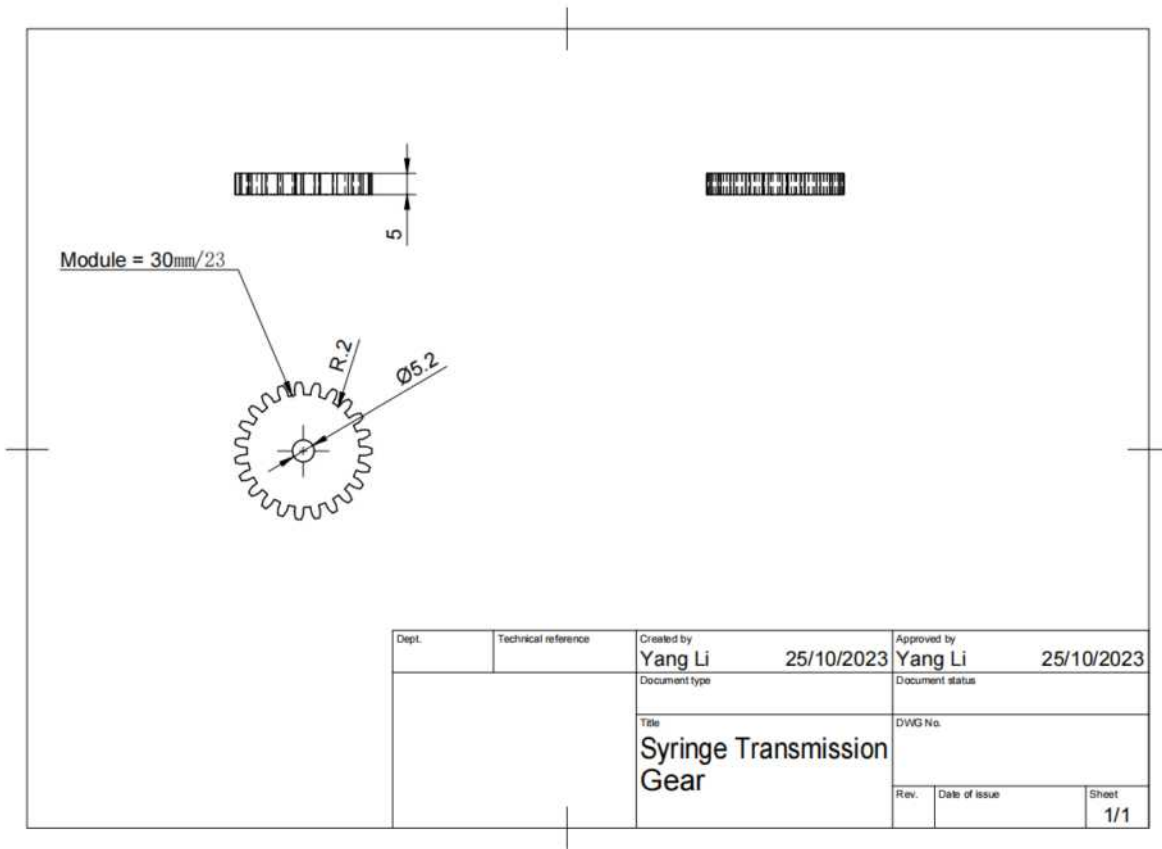
Figure 33: The Gear to transmit power from servo motor to the syringe.
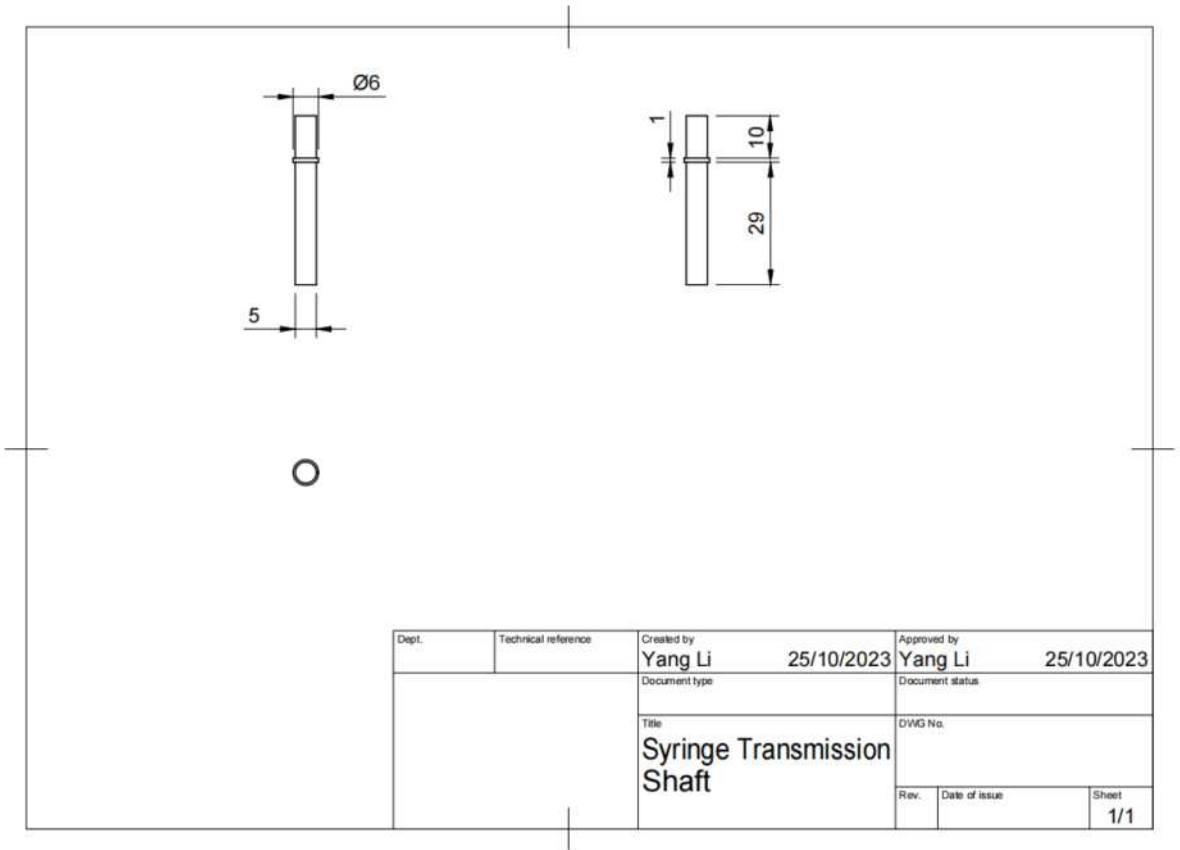
Figure 34: The shaft to attach syringe gear (Figure 32).
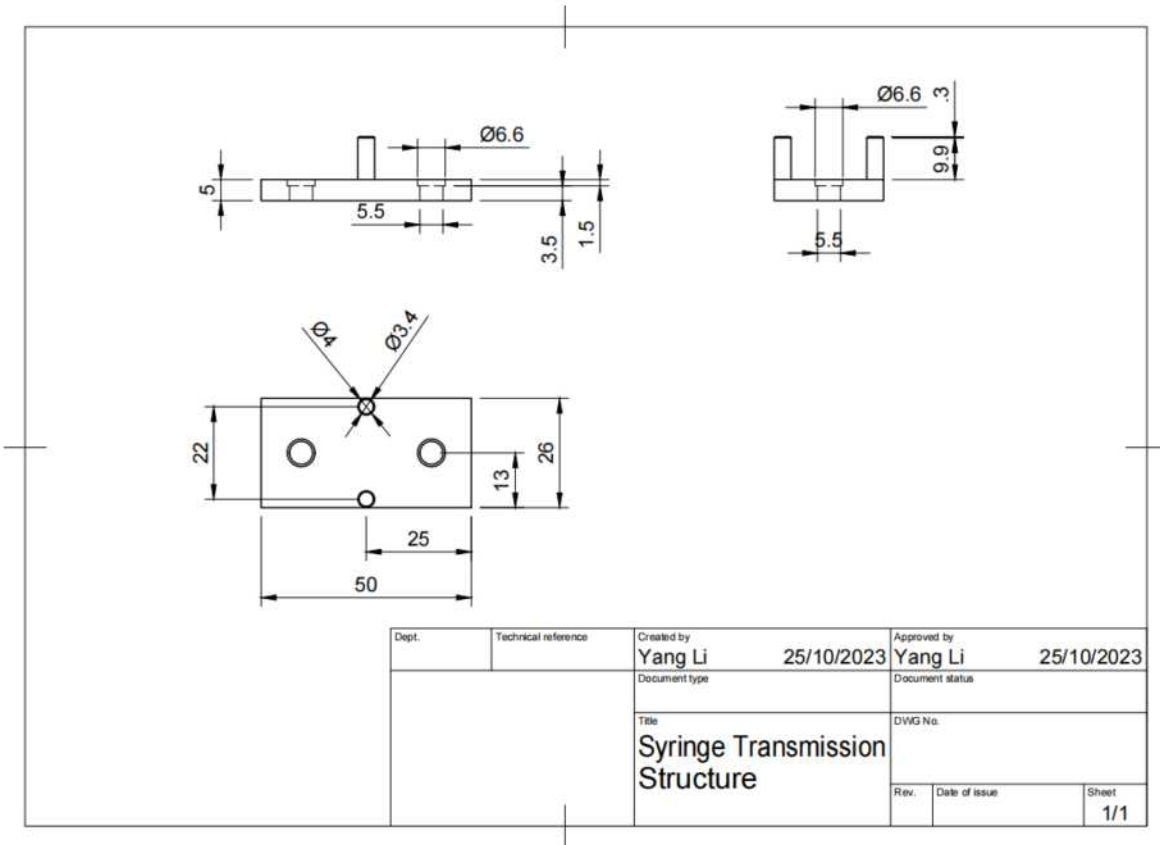
Figure 35: Pallet to hold transmission gear (Figure 33).
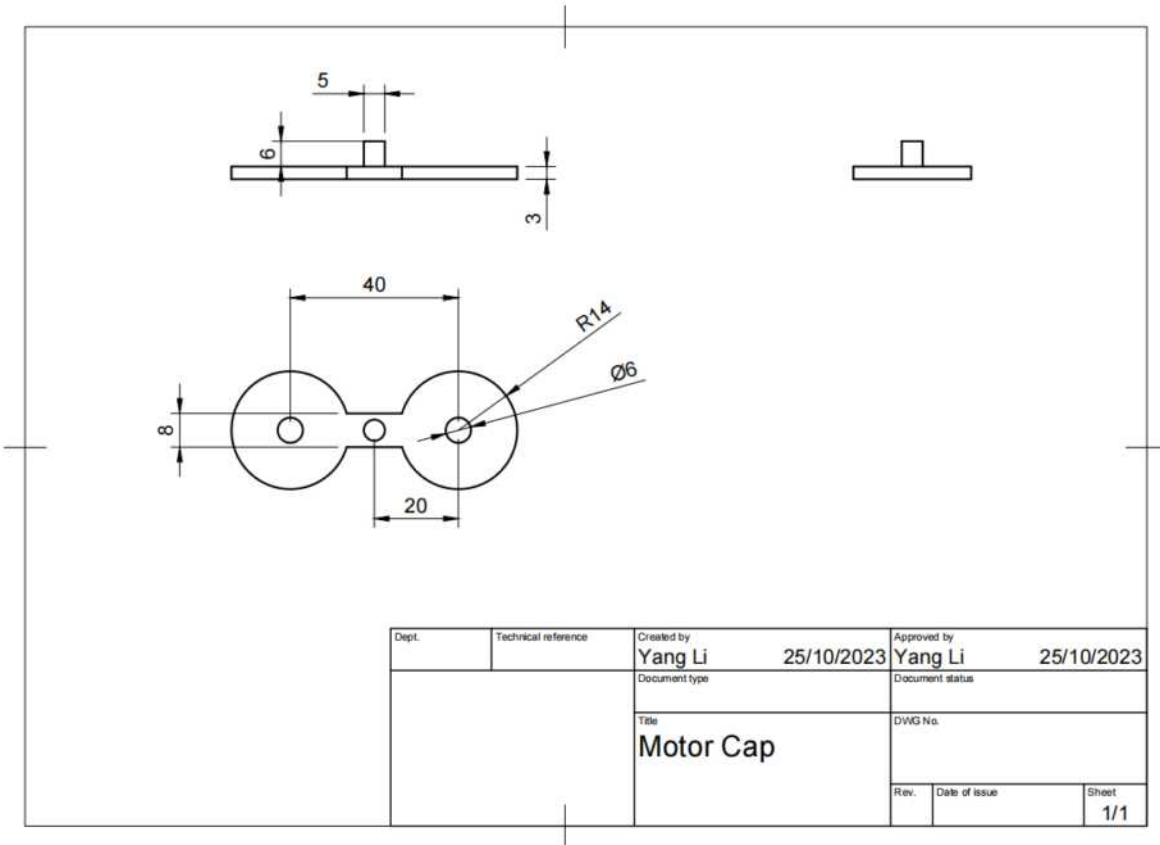
Figure 36: Pallet to hold motors.
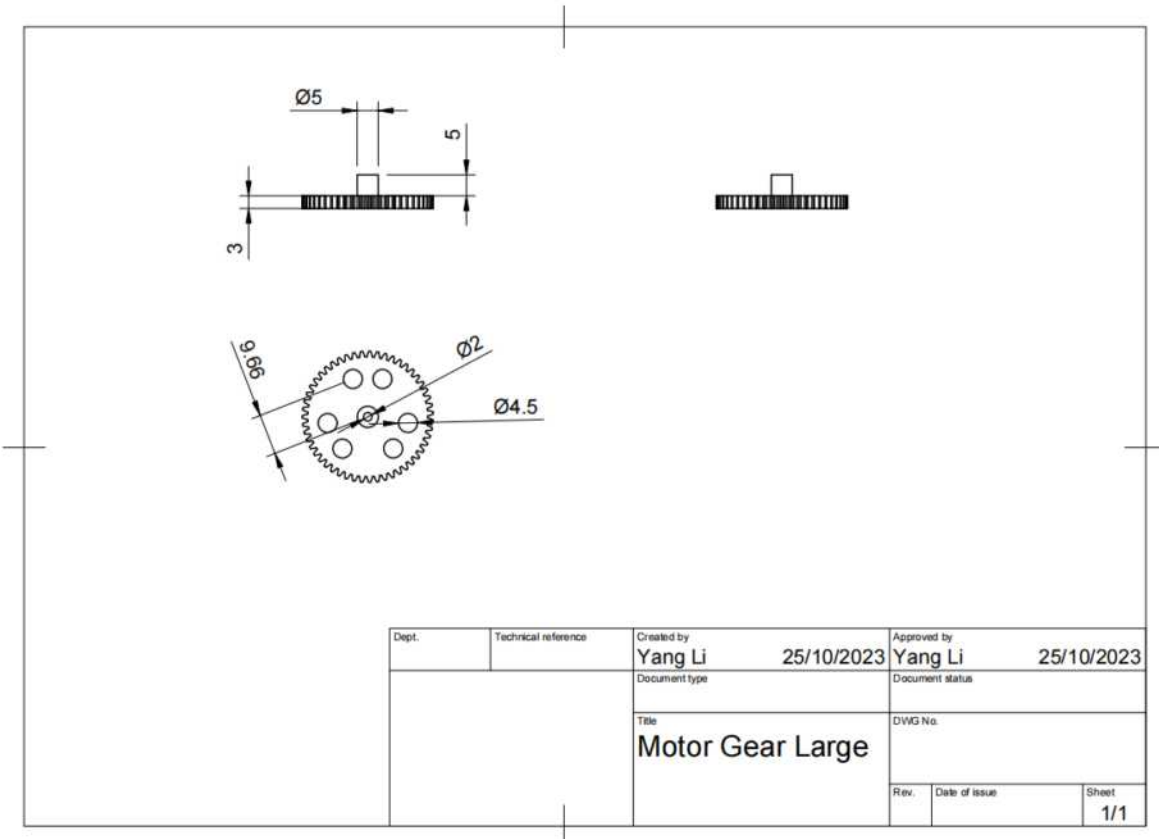
Figure 37: Driving wheel to be attached on motors
for thrusting propeller.
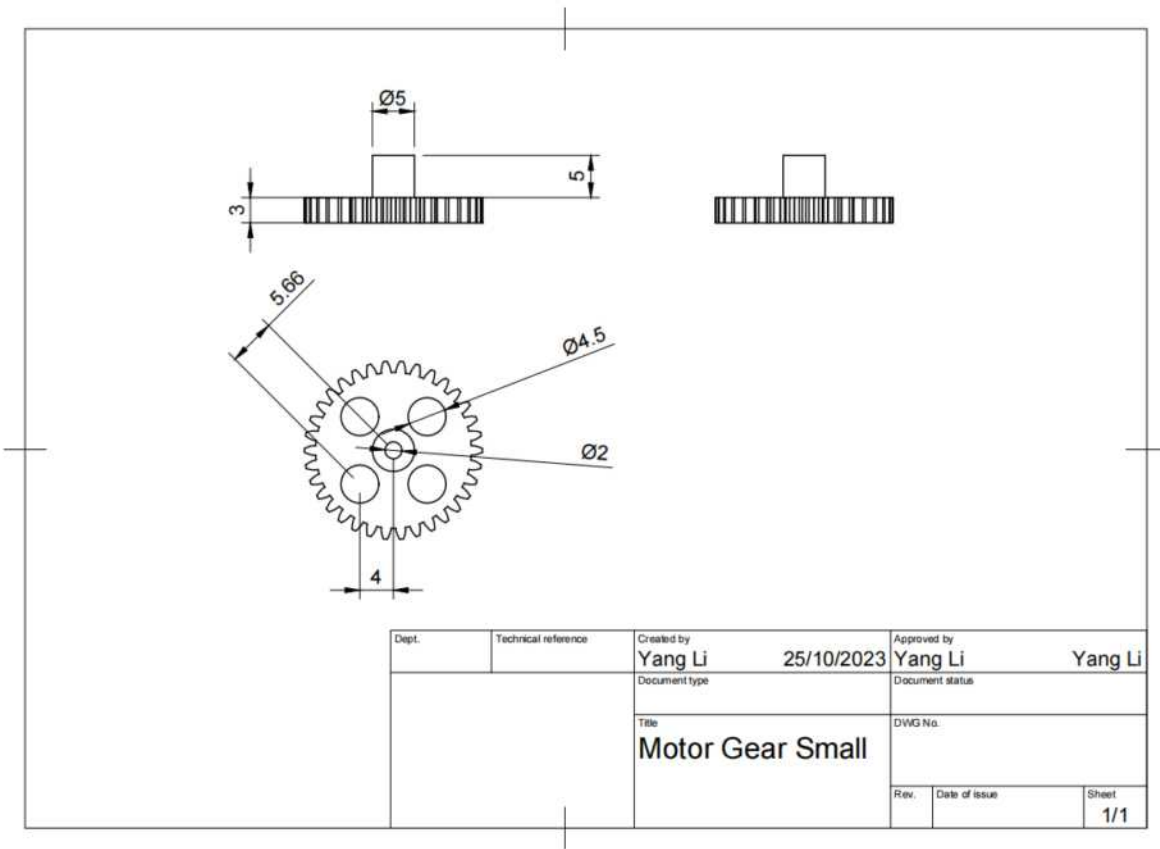
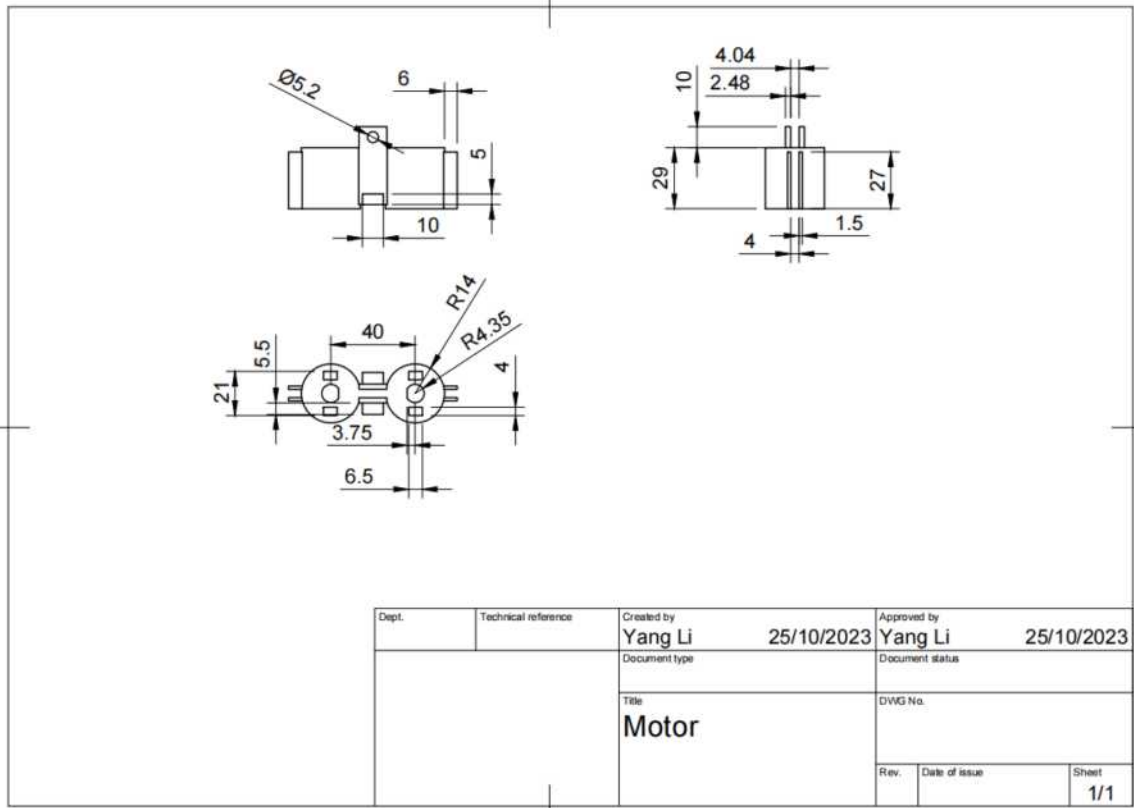Figure 38: Driving wheel to be attached on motors
for turning propeller.

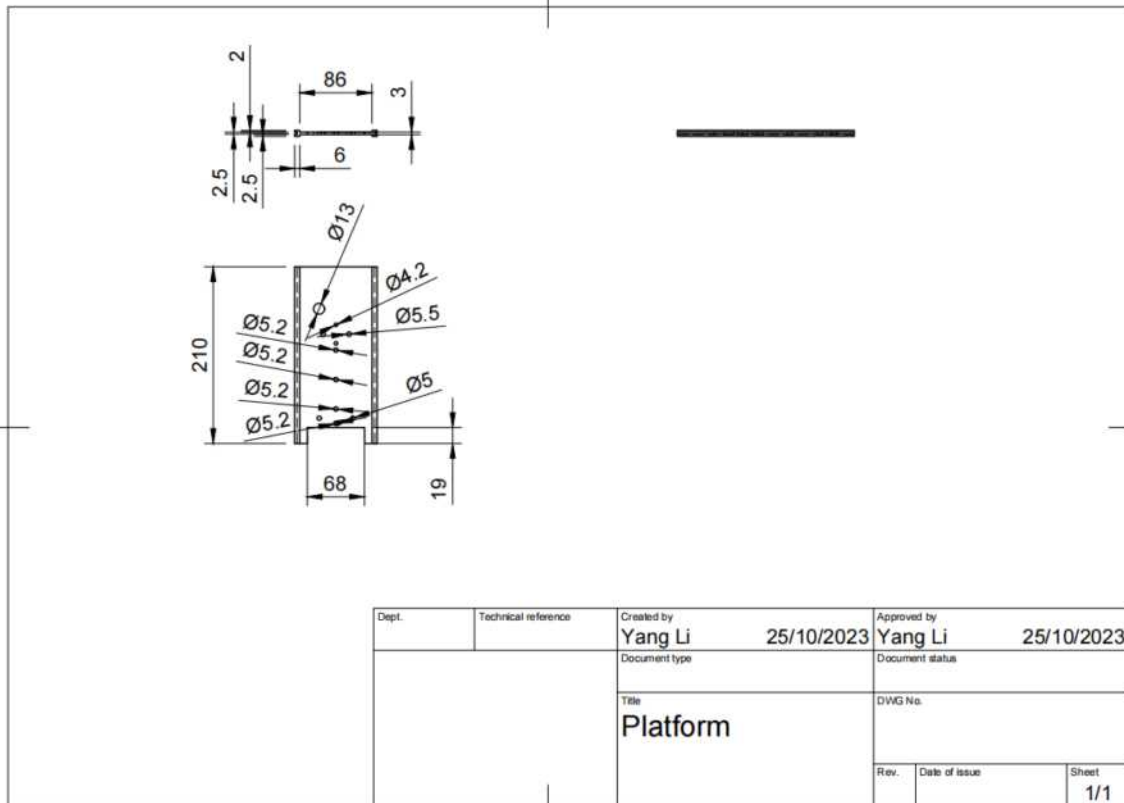Figure 39: Outer shell to hold motors.

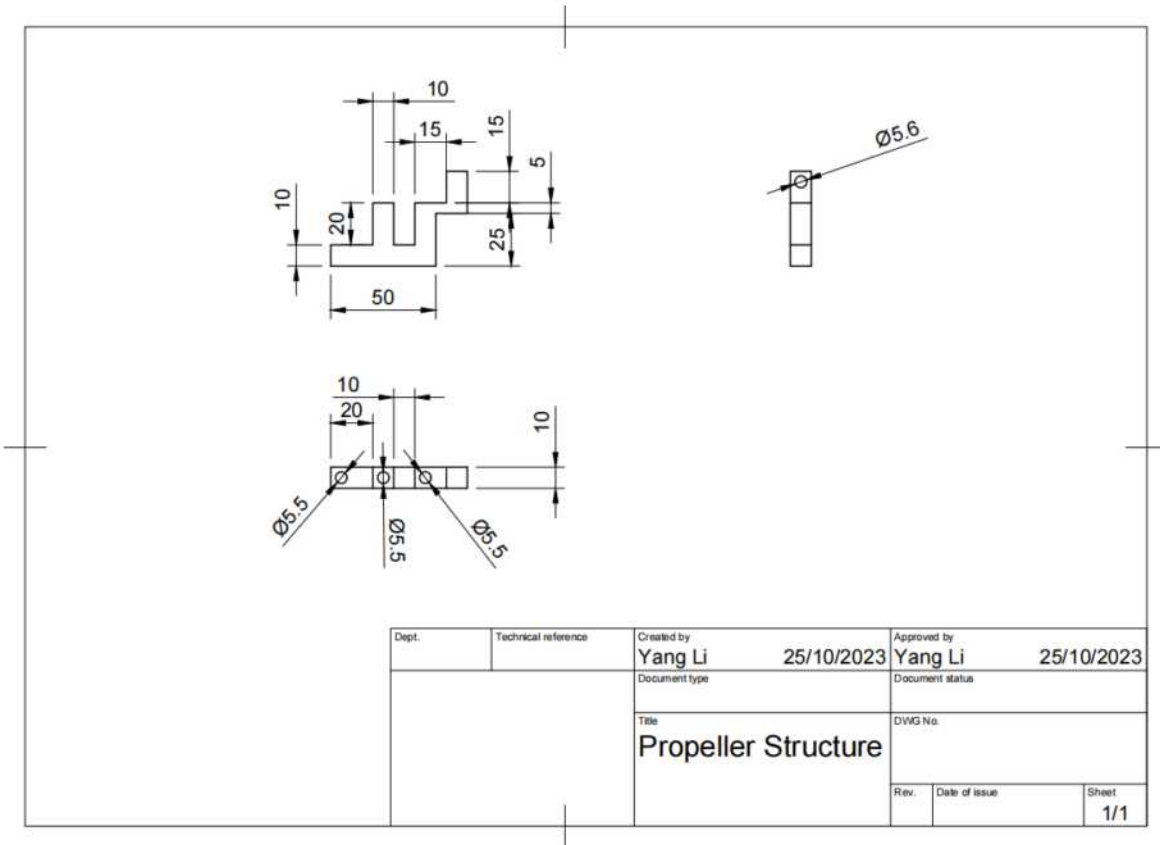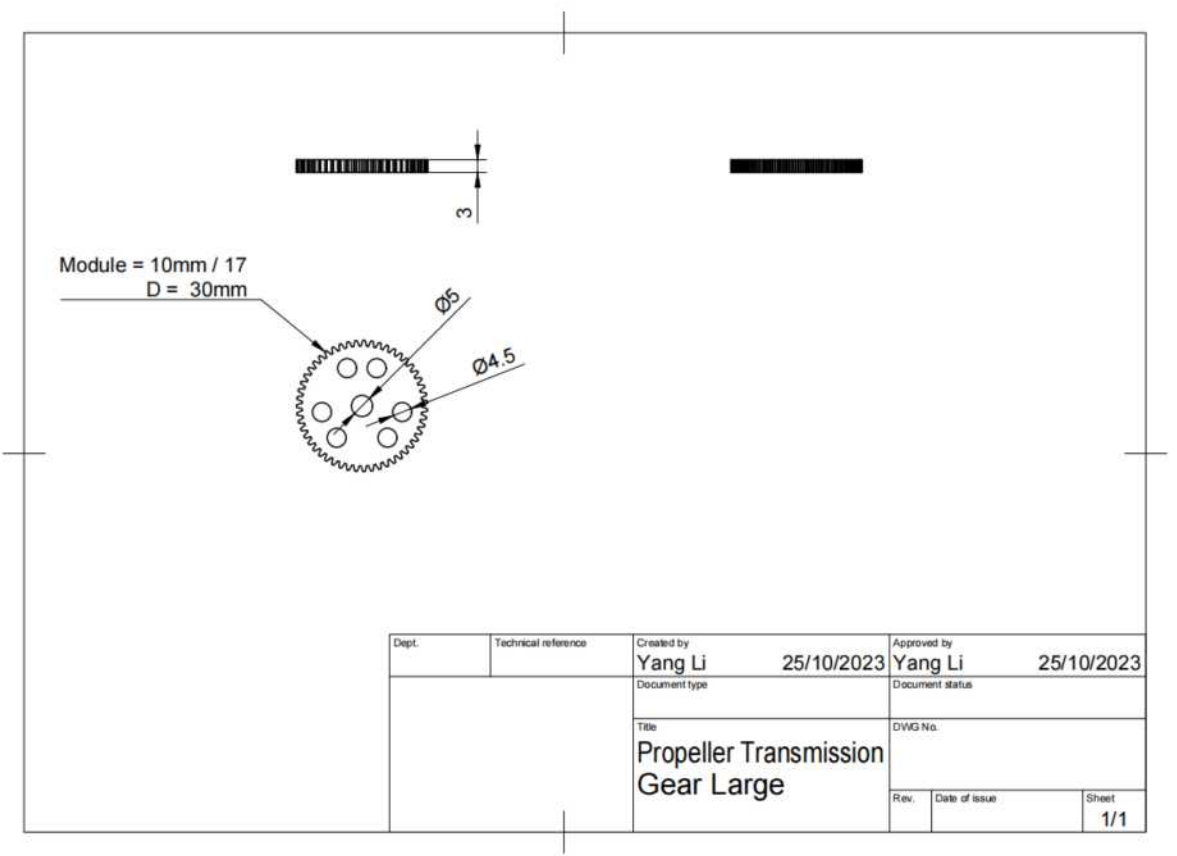Figure 40: Platform to carry all components.

Figure 41: Main body of propelling system.

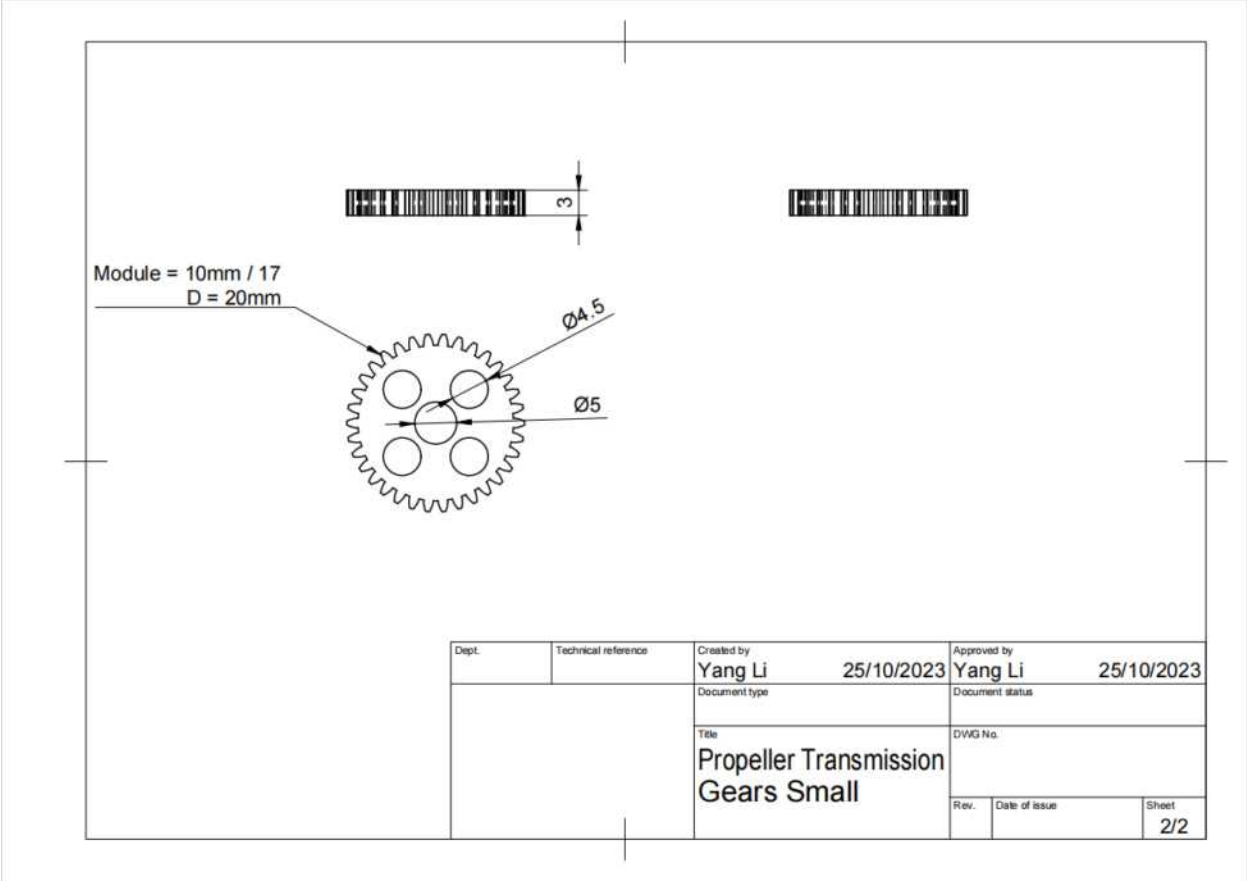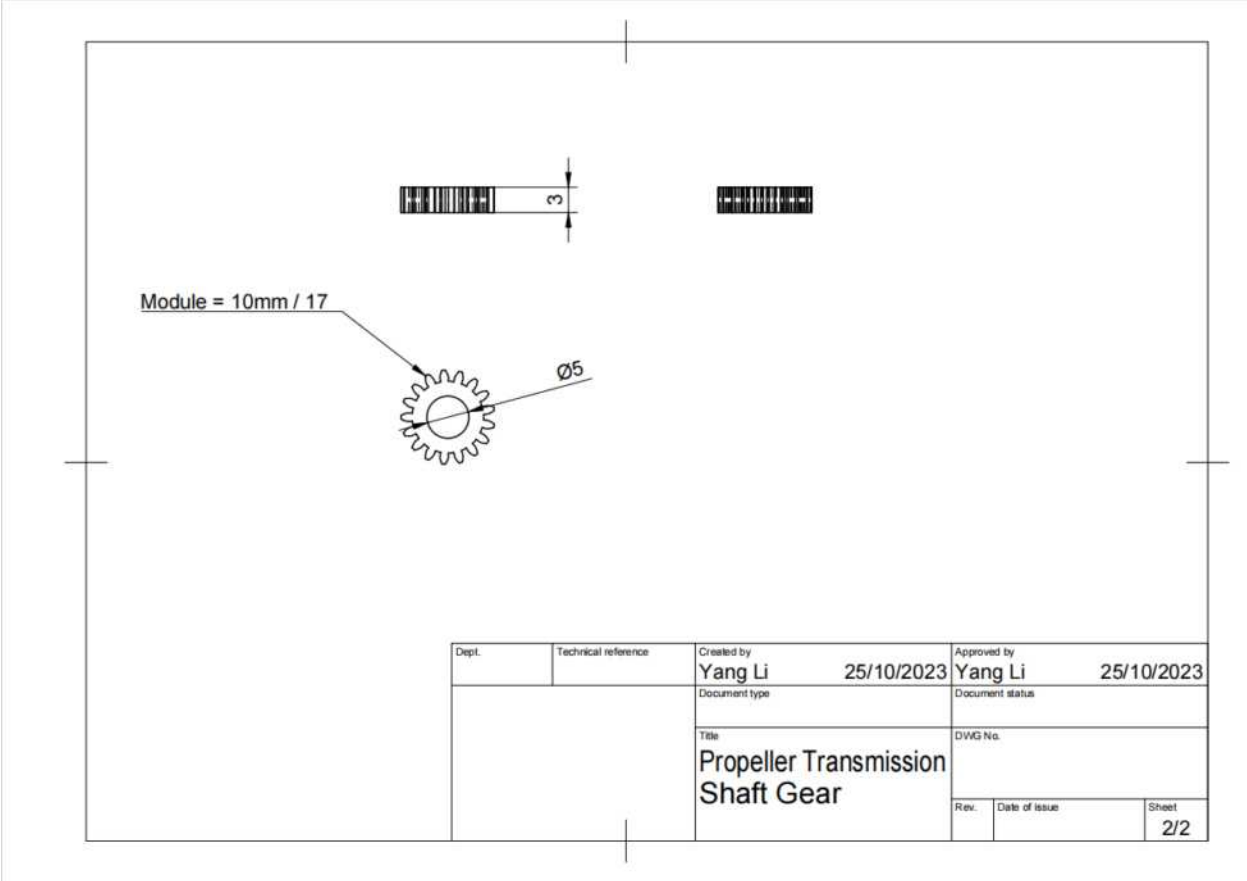Figure 42: Driving wheel to be attached on motors
for thrusting propeller.

Module = 10mm / 17
D = 20mm

Ø4.5

Ø5

3

Dept.	Technical reference	Created by		Approved by	
		Yang Li 25/10/2023		Yang Li 25/10/2023	
		Document type		Document status	
		Title		DWG No.	
		Propeller Transmission Gears Small			
				Rev. Date of issue	Sheet 2/2

Figure 43: Driving wheel to be attached on motors
for turning propeller.

Module = 10mm / 17

Ø5

3

Dept.	Technical reference	Created by		Approved by	
		Yang Li 25/10/2023		Yang Li 25/10/2023	
		Document type		Document status	
		Title		DWG No.	
		Propeller Transmission Shaft Gear			
				Rev. Date of issue	Sheet 2/2

Figure 44: Gear to transfer power from driven gear (Figure 42)
to the thrusting propeller.

Dept.	Technical reference	Created by		Approved by	
		Yang Li	25/10/2023	Yang Li	25/10/2023
		Document type		Document status	
		Title		DWG No.	
		Right-angle Gear			
				Rev.	Date of issue	Sheet
						1/1
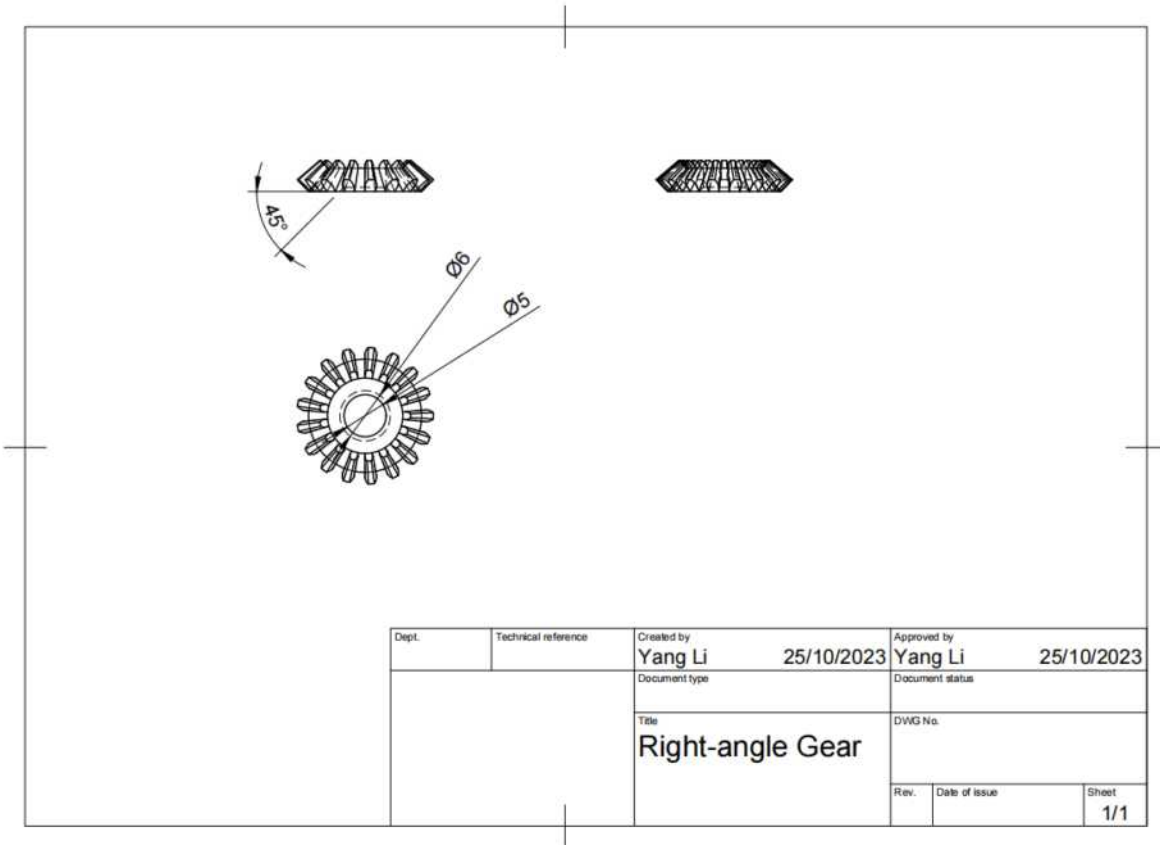
Figure 45: Angle gear to transmit power vertically
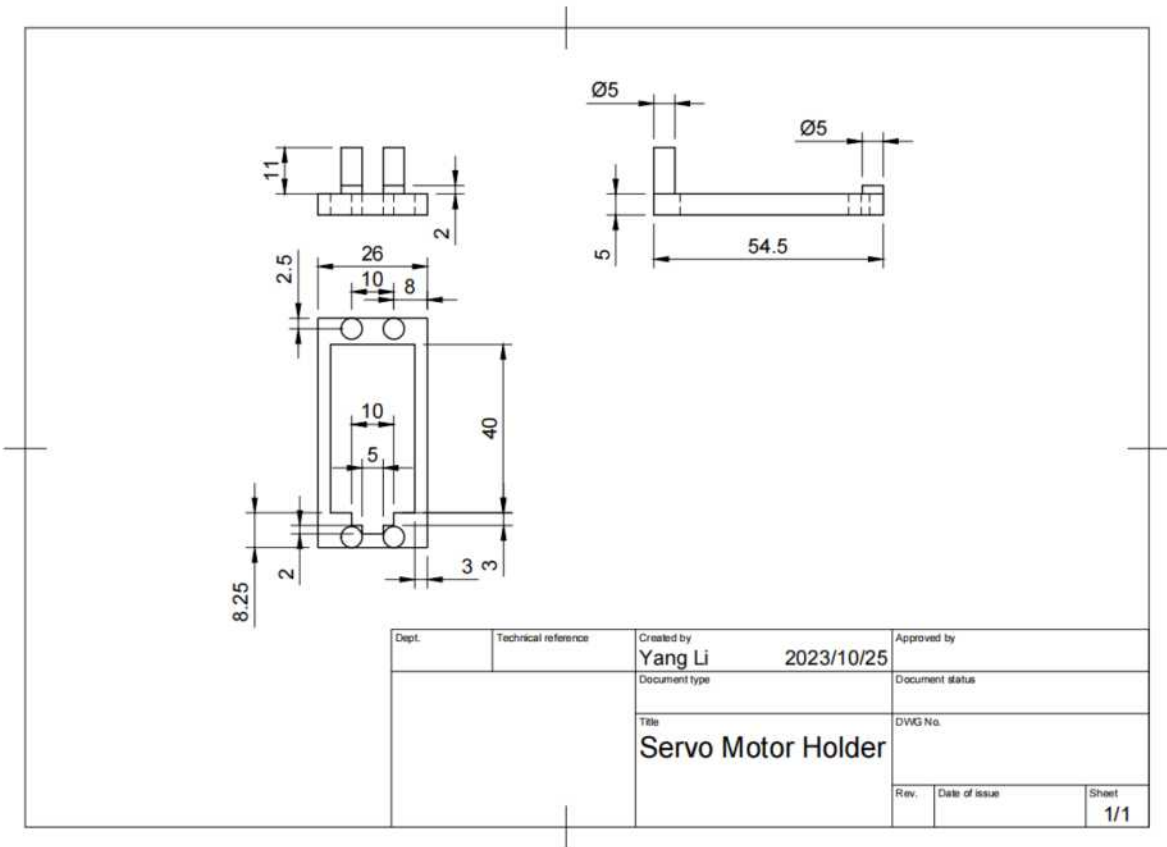for turning propeller.
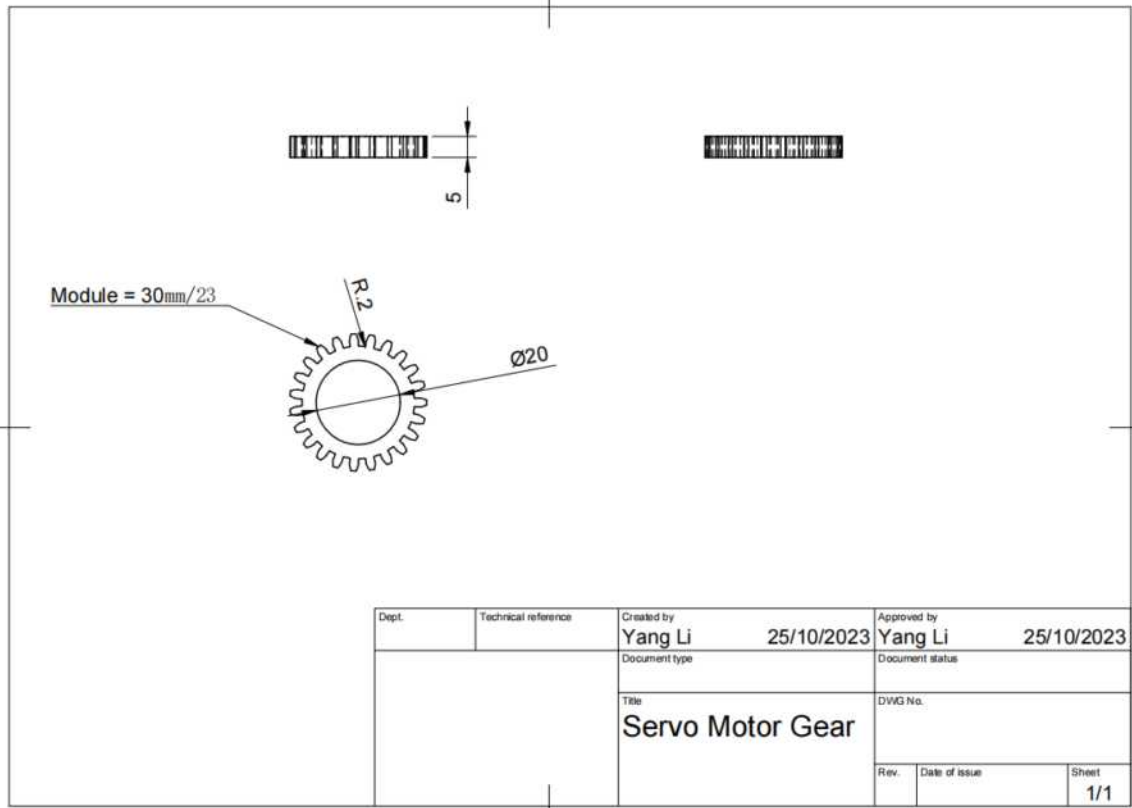
Figure 46: Gear attached on servo motor disk.

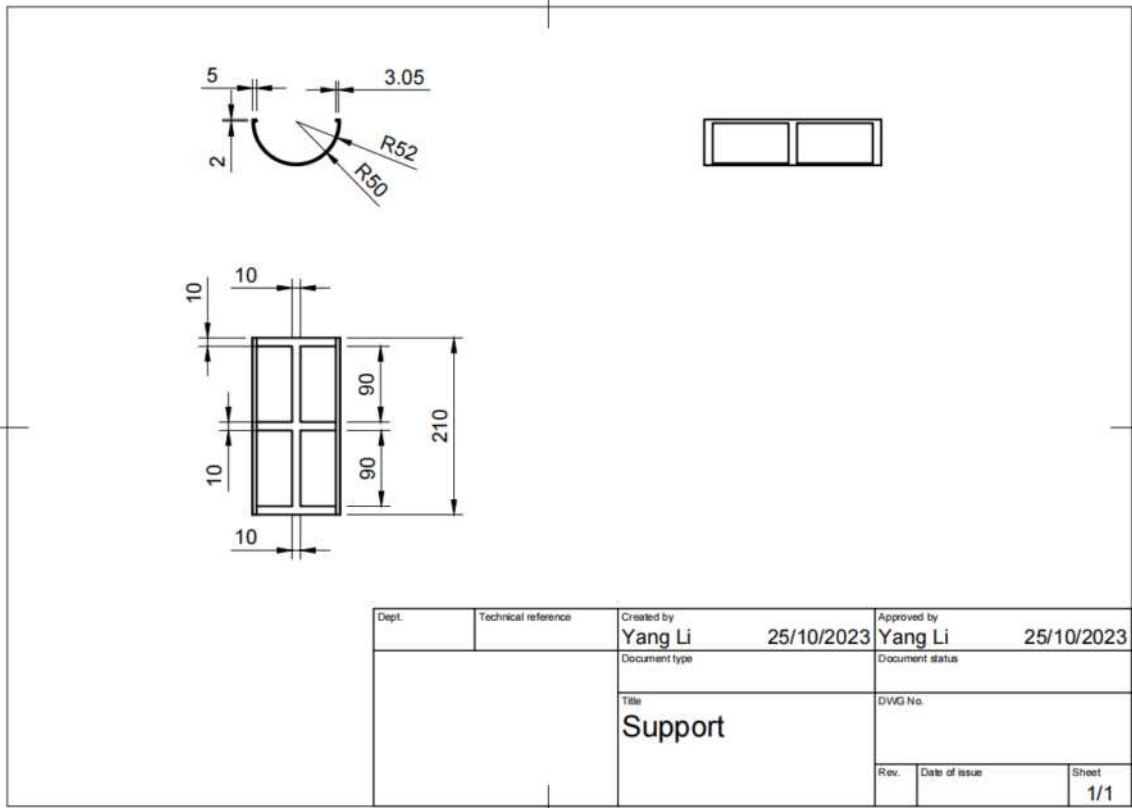Figure 47: Platform to carry all components.
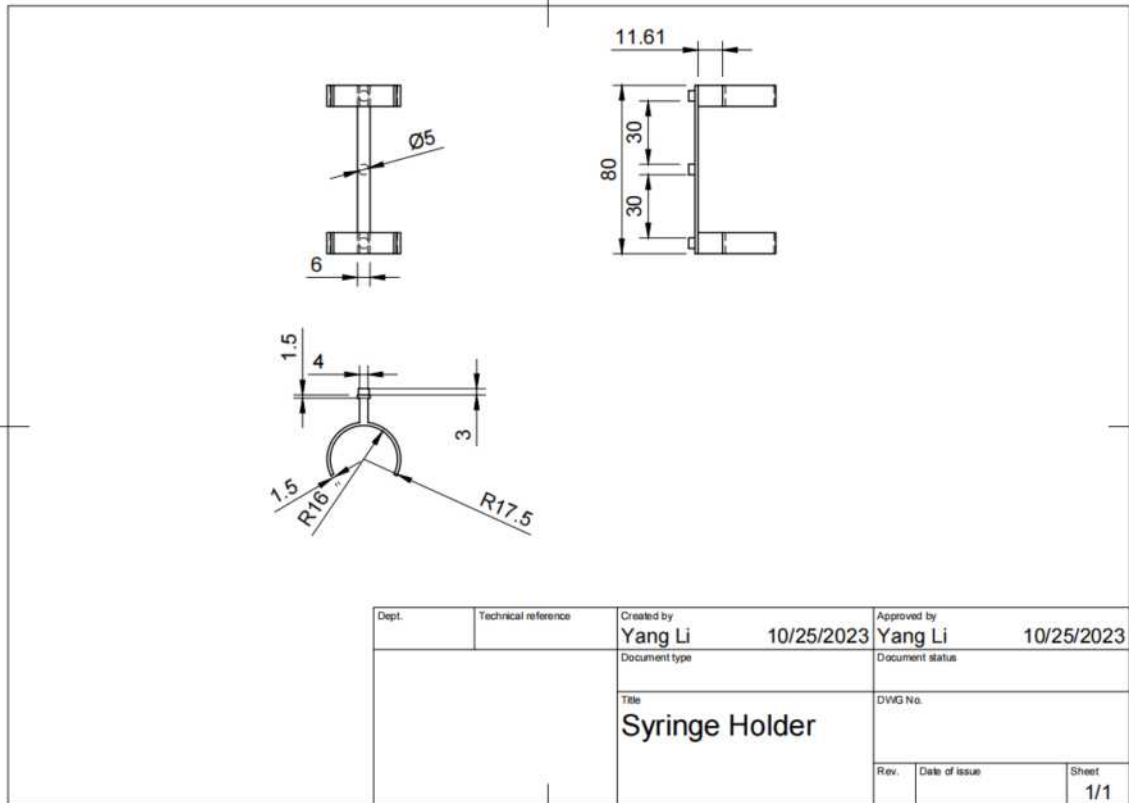
Figure 48: Structure to support the platform (Figure 40).

Figure 49: Structure to hold string in position.